**Table 1**
Profiles of the patients.

| Patients | Clinical Dx | Molecular or biochemical Dx | Age at the start of the Tx | ADL at the start of the Tx | Dose of sodium pyruvate (g/kg/day) | Duration of the Tx |
|---|---|---|---|---|---|---|
| Patient 1 | Leigh syndrome | m.8993 T>G | 8 y 4 m | Bedridden<br>Unable to roll over<br>Tube fed | 0.5 | 27 m |
| Patient 2 | Leigh syndrome | m.9176 T>C | 8 m | Bedridden<br>Unable to roll over<br>Tube fed | 0.5 | 66 m |
| Patient 3 | Non-specific encephalomyopathy | Complex I + IV deficiency | 1 y 8 m | Able to roll over to one direction<br>Unable to creep<br>Orally fed | 0.5 then 1.0 | 17 m |
| Patient 4 | Myopathic mitochondrial depletion syndrome | mtDNA depletion | 1 y 7 m | Bedridden<br>Unable to roll over<br>On a respirator<br>Tube fed | 0.5 | 41 m |

Dx, diagnosis; Tx, treatment; mt, mitochondrial; ADL, activities of daily living.

(namely, the patient with combined deficiencies of complex I and IV) were tube fed. The ages at the initiation of pyruvate therapy were 8–100 months (median 20 months). The durations of therapy were 17–66 months (median 34 months). During the pyruvate therapy monitoring period, all other concomitant mitochondrial disease medications were maintained unchanged.

### 2.2. Pyruvate

Sodium pyruvate was obtained from Musashino Chemical Laboratory (Tokyo). Sodium pyruvate was administered at 0.5 g/kg/day orally or through a feeding tube in 2 divided doses. This dose was increased to 1.0 g/kg/day in one patient. To avoid osmotic diarrhea, the pyruvate was dissolved in water at concentrations of approximately 2%–10%. Higher concentrations were utilized if the dilution caused overhydration or the volume was too large to drink.

### 2.3. Clinical evaluation

The efficacy of the pyruvate therapy was clinically evaluated with 3 standard scales: the Newcastle Pediatric Mitochondrial Disease Scale (NPMDS) [5], the Gross Motor Function Measure with 88 items (GMFM-88) [6], and the Japanese Mitochondrial Disease Rating Scale (JMDRS) [7]. The NPMDS is composed of 4 domains: Section I, current function; Section II, systemic specific involvement; Section III, current clinical assessment; and Section IV, quality of life. Sections I–III are scored based on objective observations, and Section IV takes the subjective views of the parents into account. Higher scores indicate more severe clinical situations. There are 3 sets of age-specific NPMDSs. Depending on the patient's age at the time of the evaluation, the NPMDS for 0–24 months or that for 2–11 years was used. The GMFM-88 is composed of 5 dimensions: A, lying and rolling; B, sitting; C, crawling and kneeling; D, standing; and E, walking, running and jumping. The scores are expressed in percentages relative to the maximum score in each dimension. The total score is expressed as the mean of percentages across all 5 dimensions. As the patients were bedridden, only dimensions A and B could be assessed, and the scores for the dimensions C to E were considered to be zero %. Higher scores indicate better motor abilities. The JMDRS is the modified Japanese version of the European Neuromuscular Conference (ENMC) Mitochondrial Disease Rating Scale [8]. Higher scores in this scale indicate more severe symptoms. With the exception of Patient 4, who was only assessed with the NPMDS, all other patients were evaluated with the NPMDS and the GMFM at the same time. Patient 2 was initially monitored with the JMDRS. Then, after a 4-week-washout period, the patient was reassessed with the NPMDS and GMFM. Changes in motor functions that were too subtle to be detected with these scales were descriptively recorded. Serum lactate and pyruvate levels as well as plasma amino acids were monitored.

### 2.4. Statistical analysis

Statistical analysis of the biochemical data was performed using Mann–Whitney *U*-test. A value of $p < 0.05$ was considered as statistically significant.

## 3. Results

The changes in motor function and assessment scores are summarized in Table 2.

### 3.1. Patient 1 (m.8993 T>G Leigh syndrome)

The therapy was initiated at the age of 8 years and 4 months, and at this time, this female patient was unable to roll over. In the supine position, she could not raise her legs more than 45 degrees from the floor (as measured at the hip joint). One month after the initiation of therapy, the patient gained the abilities to roll over and raise her legs vertically from the floor. The movement of her arms became more active and rapid. The overall NPMDS score changed from 42.3 to 38.6. The sum of the scores for sections I–III changed from 31 to 29, which indicates that the objective findings improved by 2 points over one month. Dimension A of the GMFM-88 also changed from 31.4% to 47.1%, which resulted in a change from 6.3% to 9.4% in the total score. Thus, this patient's improvement was confirmed semi-quantitatively with 2 scales. Next, pyruvate was withdrawn to confirm the effect of the pyruvate treatment. Within 1 to 2 weeks, the patient became lethargic and less active. After 19 days of washout, she developed status epilepticus. Resumption of pyruvate therapy restored her clinical status to the pre-washout state. Upon re-evaluation at the age of 10 years and 7 months (after 26 months of treatment excluding the washout period), the patient exhibited maintained improved motor ability as confirmed by the unchanged GMFM-88 score. The NPMDS was not administered at this point.

Blood lactate levels and lactate/pyruvate ratios measured twice during the pre-treatment period and once after the 19-day-washout were from 1.2 mM to 1.5 mM (median 1.2 mM), and from 14.2 to 25.6 (median 19.7), respectively. Those measured at 1, 4, 18 and 20 months after the treatment resumption following the washout period ranged from 0.81 mM to 1.2 mM (median 0.85 mM), and from 15.7 to 27.3 (median 20.0), respectively (Table 3). Thus, lactate levels decreased with pyruvate therapy, but the difference was not significant. Lactate/pyruvate ratio was not reduced. Plasma alanine, valine and lysine levels were measured after the washout and 1 month after the treatment resumption. None of these decreased with the therapy (Table 3).

**Table 2**
Clinical effects of pyruvate therapy.

| | | | | |
|---|---|---|---|---|
| Patient 1, Leigh syndrome with m.8993 T>G | | | | |
| | | At the Tx initiation (Age 8 y 4 M) | 1 month Tx (Age 8 y 5 m) | 26 months Tx (Age 10 y 7 m) |
| ADL | | Unable to roll over<br>Unable to raise the legs > 45° in supine position | Able to roll over<br>Able to raise the legs 90°<br>Moves arms more rapidly | The same as the ADL at 8 y 5 m |
| NPMDS | I | 18 | 18 | ND |
| | II | 2 | 1 | ND |
| | III | 11 | 10 | ND |
| | IV | 11.3 | 9.6 | ND |
| | Overall | 42.3 | 38.6 | ND |
| GMFM | A | 31.4% | 47.1% | 47.1% |
| | Total | 6.3% | 9.4% | 9.4% |
| Patient 2, Leigh syndrome with m.9176 T>C. First treatment | | | | |
| | | At the Tx initiation (Age 8 m) | 1-month Tx (Age 9 m) | 12-month Tx (Age 20 m) |
| ADL | | Unable to roll over<br>Partially tube-fed | Unable to roll over<br>Partially tube-fed | Able to roll over<br>Orally fed |
| JMDRS | | 52 | 52 | 53 |
| Patient 2. Second treatment after washout. | | | | |
| | | After 4-week washout (Age 5 y 3 m) | 2 months after the Tx resumption (Age 5 y 5 m) | 11 months after the resumption (Age 6 y 5 m) |
| ADL | | Unable to roll over<br>Tube-fed | Unable to roll over<br>Tube-fed | Unable to roll over<br>Tube-fed |
| NPMDS | I | 13 | 13 | 15 |
| | II | 3 | 3 | 5 |
| | III | 14 | 14 | 17 |
| | IV | 4.2 | 4.2 | 16.7 |
| | Overall | 34.2 | 34.2 | 53.7 |
| GMFM | A | 5.9% | 5.9% | 3.9% |
| | Total | 1.2% | 1.2% | 0.8% |
| Patient 3, complex I + IV deficiency | | | | |
| | | At the Tx initiation (Age 1 y 8 m) | 2-month Tx (1 y 10 m) | 12-month Tx (2 y 8 m) |
| ADL | | Roll over one direction<br>Head control fair<br>Mild dysphagia | Roll over bilaterally<br>Head control fair<br>No dysphagia | Roll over bilaterally<br>Head control poor |
| NPMDS | I | 7 | 6 | 6 |
| | II | 6 | 6 | 2 |
| | III | 15 | 13 | 13 |
| | IV | 16.7 | 7.3 | 7.3 |
| | Overall | 44.7 | 32.3 | 28.3 |
| GMFM | A | 54.9% | 66.7% | 60.8% |
| | B | 13.3% | 13.3% | 3.3% |
| | Total | 13.6% | 16.0% | 12.8% |
| Patient 4, mitochondrial DNA depletion syndrome | | | | |
| | | At the Tx initiation (Age 1 y 7 m) | 2-month Tx (Age 1 y 9 m) | 41-month Tx (Age 5 y 0 m) |
| ADL | | On respirator<br>Unable to raise the forearm above the floor<br>Myopathy only | On respirator<br>Able to raise the forearm 90° at the elbow.<br>Myopathy only | On respirator<br>Unable to raise the forearm<br>Encephalomyopathy |
| NPMDS | I | 7 | 7 | 15 |
| | II | 6 | 6 | 15 |
| | III | 5 | 5 | 24 |
| | IV | 17 | 13 | 10.8 |
| | Overall | 35 | 31 | 64.8 |

Tx, treatment; ADL, Activities of daily living; NPMDS, Newcastle Pediatric Mitochondrial Disease Scale; GMFM, Gross Motor Function Measure; JMDRS, Japanese Mitochondrial Disease Rating Scale; I–IV, Sections I–IV of NPMDS; A and B, Dimensions A and B of GMFM; ND, not done.

### *3.2. Patient 2 (m.9176 T>C Leigh syndrome)*

Pyruvate therapy was initiated at the age of 8 months for this male patient who was unable to roll over and had poor head control. Oral feeding was partially possible. After one-month of treatment, motor function was not altered and neither was the JMDRS score, which was 52. After 12 months of treatment, at the age of 1 year and 8 months, the patient was able to roll over and full oral feeding became possible. However, these subtle changes were not detected by JMDRS. The JMDRS score actually increased by 1 point due to seizures. At 3 years

**Table 3**
Changes in blood lactate and amino acids levels with pyruvate therapy.

| | Lactate (mM) Median (range) (n) (normal: 0.3–1.9) | | Lactate/Pyruvate ratio Median (range) (n) (normal: 10–15) | | Alanine (μM) Median (range) (n) (normal: 209–523) | | Valine (μM) Median (range) (n) (normal: 148–307) | | Lysine (μM) Median (range) (n) (normal: 109–242) | |
|---|---|---|---|---|---|---|---|---|---|---|
| | Before | After | Before | After | Before | After | Before | After | Before | After |
| Patient 1 | 1.2 (1.2–1.5) (3) | 0.85 (0.81–1.2) (4) | 19.7 (14.2–25.6) (3) | 20.0 (15.7–27.3) (4) | 256 (1) | 439 (1) | 165 (1) | 263 (1) | 104 (1) | 200 (1) |
| Patient 2 | 2.8 (1.2–4.4) (2) | 2.4 (0.9–3.1) (5) | 23.2 (19.2–27.2) (2) | 23.1 (14.7–30.5) (5) | 402 (360–443) (2) | 340 (320–428) (5) | 173 (172–174) (2) | 168 (135–171) (5) | 139 (96.6–180) (2) | 112 (96.2–172) (5) |
| Patient 3 | 3.9 (2.5–8.0) (4) | 5.6 (3.7–9.3) (7) | 25.0 (14.7–35.3) (4) | 30.5 (17.7–45.9) (7) | 543 (427–659) (2) | 729 (549–840) (7) | 171 (154–188) (2) | 219 (149–280) (7) | 117 (87.8–146) (2) | 122 (88.7–172) (7) |
| Patient 4 | 2.3 (2.1–2.7) (4) | 2.5 (2.3–2.7) (5) | 16.9 (14.9–18.7) (4) | 17.3 (14.1–21.2) (5) | 350 (1) | 384 (381–386) (2) | 140 (1) | 187 (182–191) (2) | 108 (1) | 158 (157–158) (2) |

Mann–Whitney U-test did not show any significant differences.

of age, the patient developed acute encephalopathy associated with a viral infection and lost the abilities of oral feeding and rolling over. To re-evaluate the efficacy of pyruvate, the patient was reassessed with the NPMDS and GMFM-88 at the age of 5 years and 3 months after a 4-week pyruvate washout period. The washout did not cause any deterioration. Two months after the resumption of the pyruvate therapy, neither the NPMDS (overall score, 34.2) nor the GMFM-88 (total score 1.2%) scores changed. After 11 months of therapy after the washout, the scores for all sections of the NPMDS increased, and the overall score increased by 19.5 points. The total GMFM-88 score decreased from 1.2% to 0.8%. Thus, pyruvate was not effective for this patient.

Blood lactate levels and lactate/pyruvate ratios measured twice during 2 months before the first pyruvate therapy at the age of 8 months were 1.2 mM and 4.4 mM (median, 2.8 mM), and 19.2 and 27.2 (median, 23.2), respectively. Those at 1, 2, 3, 4 and 12 months after the therapy ranged from 0.9 mM to 3.1 mM (median, 2.4 mM) and from 14.7 to 30.5 (median, 23.1), respectively. Lactate levels and lactate/pyruvate ratios did not change significantly with the therapy (Table 3). Plasma alanine, valine and lysine levels measured twice before and at 1, 2, 3, 4 and 12 months after the therapy showed a mild but non-significant decrease with the therapy (Table 3).

### 3.3. Patient 3 (combined deficiencies of complex I and IV)

This male patient presented with developmental delay, nystagmus, hypertrophic cardiomyopathy and mild hearing disturbance (38 dB). At the age of 11 months, he developed status epileptics followed by regression. Increased lactate levels and lactate/pyruvate ratio in the cerebrospinal fluid (CSF) (lactate:5.2 mM, lactate/pyruvate ratio: 20.0) and blood (lactate: 12.3 mM, lactate/pyruvate ratio: 41.6) led to a skin biopsy, which revealed deficiencies in complexes I and IV: the activities of complex I and IV relative to the activity of citrate synthase were 24.7% and 22.9% of normal controls (n = 12), respectively, and those relative to the activity of complex II were 33.5% and 31.4% of normal, respectively. Muscle biopsy could not be obtained. The clinical signs and symptoms fulfilled the mitochondrial disease criteria for definite mitochondrial disorder proposed by Morava et al. [9]. No mutation was revealed in the mitochondrial DNA. Molecular analysis of the nuclear genes is under way. Treatment with coenzyme $Q_{10}$ at the age of 1 year and 6 months did not produce any improvement. Pyruvate therapy was initiated at the age of 1 year and 8 months, and at this time the patient had mild dysphagia and incomplete head-control. He could roll over only in one direction. After 2 months of pyruvate therapy with a maintenance dose of 1.0 g/kg/day, he gained the ability to roll over bilaterally and the dysphagia disappeared. The total scores for sections I–III decreased from 28 to 25, and the score for IV also decreased from 16.7 to 7.3. The GMFM-88 score increased from 13.6% to 16.0%. Thus, the efficacy of the 2-month pyruvate therapy was confirmed by both scales. However, over the next 10 months, a slow regression in motor function was observed, and at 2 years and 8 months of age (after 12 months of treatment), this patient's GMFM-88 score decreased from 16.0% to 12.8%. However, the scores for section II of the NPMDS (the version for 2–11 year-olds was used) decreased by 4 points due to improvements in seizures and gastrointestinal and hepatic function. The regression of motor function that was evident in the GMFM-88 was not detected by the NPMDS (the scores for sections I and III were unchanged).

Blood lactate levels and lactate/pyruvate ratios measured 4 times during the 9-month pre-treatment period ranged from 2.5 mM to 8.0 mM (median, 3.9 mM), and from 14.7 to 35.3 (median, 25.0), respectively. Those measured 1, 2, 3, 4, 6, 9 and 12 months after the therapy ranged from 3.7 mM to 9.3 mM (median, 5.6 mM), and from 17.7 to 45.9 (median 30.5), respectively (Table 3). Thus, neither the blood lactate levels nor the lactate/pyruvate ratios decreased with the pyruvate therapy. Among the measurements, those measured twice during the first 2-month treatment, which was clinically effective, did not show any decrease either. Plasma alanine, valine and lysine levels were

measured twice before the treatment and 7 times after the therapy. None of these decreased significantly with the therapy (Table 3).

Throughout the therapy, the patient exhibited chronic diarrhea that seemed to be a side effect of the treatment.

### 3.4. Patient 4 (myopathic form of the mtDNA depletion syndrome)

The short-term efficacy of pyruvate therapy for this female patient and her clinical and biochemical profile have been reported in detail elsewhere [3]. Briefly, the patient developed severe generalized weakness including facial muscles and respiratory failure during the neonatal period. The patient had a tracheostomy and was on a respirator. She had lactic acidosis (3.0 mM to 6.5 mM) with high lactate/pyruvate ratio (36 to 97). Muscle biopsy revealed ragged red fibers and decreased cytochrome c oxidase staining. The activities of complex I, III and IV relative to the activity of citrate synthase in the muscle were 10.6%, 26.7% and 14.1% of the control, respectively. Those relative to the activity of complex II were 6.5%, 16.4% and 8.8%, respectively. Quantitative analysis of the mtDNA revealed that the copy number of the mitochondrial ND1 subunit relative to the nuclear CFTR gene was 35.3% (normal: >40%). Exome sequencing is under way to detect a mutation in causative genes. The clinical signs and symptoms were compatible with Morava et al.'s criteria for definite mitochondrial disease [9]. As reported elsewhere, after 2 months of pyruvate therapy, the patient exhibited a mild improvement in the movement of her extremities at the age of 1 year and 9 months [3]. The overall NPMDS scores decreased from 35 to 31, but this decrease was limited to section IV. As the patient was not assessed with the GMFM, we were unable to semi-quantitatively demonstrate the improvement in motor function. One month later (after 3 months of treatment), the patient developed status epilepticus. An MRI revealed lesions in the occipital areas, which indicated a progression from the myopathic form to the encephalomyopathic form. At 5 years of age, after 41 months of treatment, scores in all sections of the NPMDS increased, and the increase in overall NPMDS score was 33.8 points compared to the score at the 2-month treatment.

Blood lactate and lactate/pyruvate ratios measured 4 times during the 2-month pre-treatment period ranged from 2.1 mM to 2.7 mM (median, 2.3 mM), and from 14.9 to 18.7 (median, 16.9), respectively. Those measured 1, 4, 6, 8 and 13 weeks after the therapy ranged from 2.3 mM to 2.7 mM (median, 2.5 mM), and from 14.1 to 21.2 (median, 17.3), respectively (Table 3). Plasma alanine, valine and lysine levels were measured once before the therapy and 4 and 8 weeks after the therapy. None of these decreased with the pyruvate therapy (Table 3).

## 4. Discussion

All 4 of the treated patients were severely disabled and bedridden. Therefore, objective and semi-quantitative assessments of the outcomes were difficult because the expected improvements were subtle. The NPMDS is a scale that was designed to specifically monitor mitochondrial disease, which results in a variety of multi-organ symptoms. Therefore, the scale encompasses all aspects of mitochondrial disease. Consequently, this scale cannot detect small changes in motor function. The logic applies to the JMDRS. In contrast, the GMFM-88 evaluates motor function with as many as 88 items; therefore, this assessment may detect small changes in motor abilities. However, the GMFM was designed to assess cerebral palsy, and its reliability in monitoring mitochondrial disease has not been validated. In contrast to the GMFM-66, which can only be used for cerebral palsy, the GMFM-88 has been validated for the monitoring of motor functions in disorders other than cerebral palsy, such as spinal muscular atrophy, Down syndrome and traumatic brain injuries. [10–12] Therefore, we assumed that the GMFM-88 could also be used to monitor motor functions in mitochondrial disease. Nevertheless, given that the GMFM-88 has not been validated for using in mitochondrial disease, we assessed the outcomes via a combination of the GMFM-88 and NPMDS scores with the exception of patient 4, who was assessed only with the NPMDS. We also tried using other scales including Pediatric Evaluation of Disability Inventory (PEDI) [13] and Functional Independence Measure for Children (Wee-FIM) [14]. Our preliminary study, however, showed that these could not detect clinical changes in our patients.

Patients 3 and 4 were assessed with 2 different sets of age-specific NPMDSs as they matured into ages suitable for the application of the older age-specific NPMDSs during the monitoring period. The number of items scored in each section of the NPMDS for 2–11-year-olds is greater than that of the NPMDS for 0–24-month-olds. Therefore, it is possible that total NPMDS scores may increase when the version for older patients is used even if clinical severity remains unchanged. In Patient 3, the score for section II as assessed 2 years and 8 months decreased compared to the score assessed at 1 year and 10 months, whereas the scores for the other sections remained unchanged. Thus, a "pseudo-increase" in the score due to the use of a different set of NPMDS scales did not occur in this patient. In Patient 4, the scores for sections I, II and III increased by 8, 9 and 19 points, respectively, at 5 years of age compared to the scores observed at 21 months of age. Given that the maximum scores for sections I, II and III are higher by 6, 3 and 6 points, respectively, in the NPMDS for 2-11 year-olds than in the NPMDS for 0–24 month-olds, the increases in the scores that were higher than the maximum possible increases due to the differences in the versions of the NPMDS indicated that the increases were real.

The most noteworthy result of this study was that 3 of the 4 severely disabled patients (Patients 1, 3 and 4) exhibited improvement within 1 to 2 months of the initiation of pyruvate therapy. These improvements were confirmed by both the NPMDS and GMFM-88 (Patients 1 and 3) or the NPMDS only (Patient 4). The semi-quantitative improvement observed in Patient 4 was limited to section IV of the NPMDS, which accounts for the parents' subjective assessments. However, a descriptive observation record also revealed improvement in muscle power. [3] Given that no improvements were observed prior to pyruvate therapy in these patients and that the improvements were observed with 1–2 months of the initiation of pyruvate therapy, it is unlikely that the observed ameliorations were simply due to natural motor development rather than the effects of the therapy. The efficacy was particularly evident in Patient 1 who had m.8993 T>G and exhibited improvements in motor function that were maintained for over 2 years. The worsening of symptoms during pyruvate withdrawal also supported the efficacy of pyruvate treatment in this patient. In contrast, 2 of the 3 responsive patients did not maintain the improvements for longer than several months. Notably however, the overall NPMDS score for Patient 3 decreased (i.e., symptoms improved) after 12 months of therapy compared to this patient's score after 2 months of the therapy despite the worsening of the GMFM score. These findings indicated that the patient's overall health improved during long-term therapy, although this patient's motor abilities regressed. In Patient 4, the disease progression overwhelmed the effect of the pyruvate therapy shortly after the responsiveness was confirmed after 2 months of therapy; this finding indicated a limitation of this therapy. We could not explain why Patient 2, who had m.9176 T>C, did not respond to pyruvate therapy. Given the age of this patient, the mild improvements in motor function after 12 months of pyruvate therapy, which could not be detected with the JMDRS, seemed to be due to natural motor development rather than resulting from the treatment.

The only adverse effect of pyruvate therapy was the mild but chronic diarrhea that was observed in one patient who was on 1.0 g/kg/day of sodium pyruvate.

An *in vitro* study that utilized cybrid cells harboring MELAS m.3243A>G mutant mitochondria found that pyruvate treatment facilitates the pyruvate-to-lactate conversion, decreases the lactate/pyruvate ratio, normalizes the NADH/$NAD^+$ ratio, and enhances ATP production and energy charge without significantly altering the intracellular lactate level. [15] These data support the theory that the effects of pyruvate

therapy are mediated via the normalization of the NADH/$NAD^+$ ratio, which provides the $NAD^+$ that is deficient in OXPHOS disturbances. In contrast to the theory and the result of this *in vitro* study, none of our responsive patients exhibited decreases in blood lactate/pyruvate ratios, which are equivalent to the NADH/$NAD^+$ ratios, during the effective short-term therapy. Blood lactate levels decreased in 2 patients, especially in Patient 1, but the differences were non-significant. Thus, the blood lactate/pyruvate ratios and blood lactate levels of our patients could not be used as biochemical markers to monitor the effects of the therapy. The discrepancy between the clinical data from our patients and the *in vitro* data may be partly explained by the fact that blood lactate levels vary depending on the physical activity of the patient at the time of blood sampling, the interval between meal and sampling, as well as on the time required for the blood sampling procedure. However, all of our patients were bedridden and the data were from multiple samplings in different days. The blood samplings were done either after overnight-fast or several hours after a meal. Therefore, it is unlikely that the discrepancy was artifactual. Still, monitoring the lactate levels and lactate/pyruvate ratios in the CSF rather than in the blood would further reduce the possible artifact. Komaki et al. treated an ambulatory patient with Leigh syndrome associated with cytochrome c oxidase deficiency [2]. With pyruvate therapy, blood lactate level and lactate/pyruvate ratio decreased from 2.3 mM to 1.1 mM, and from 17.7 to 11.4, respectively. However, the measurements were done only once before and after the therapy, so the statistical significance could not be evaluated. Koga et al. found statistically significant decreases in blood lactate, pyruvate and alanine levels with pyruvate therapy in a non-ambulatory patient with pyruvate dehydrogenase (PDH) deficiency [4]. Blood lactate/pyruvate ratio in this patient also decreased, but the difference was non-significant (the ratios in PDH deficiency are generally normal). Differences between Komaki et al. and Koga et al.'s patients from ours were that 1) Komaki et al.'s patient was ambulatory, and 2) the pre-treatment blood levels of lactate and alanine in Koga et al.'s patient were much higher than those in our patients: the blood lactate and alanine levels in this patient were $9.6 \pm 0.54$ mM ($n = 8$) and $1700 \pm 280$ μM ($n = 8$), respectively, while the median values of pre-treatment lactate levels in our 4 patients ranged from 1.2 to 3.9 mM and those of alanine were from 256 to 543 μM. This may indicate that the blood lactate and alanine levels and lactate/pyruvate ratio are not sensitive biochemical markers to monitor the pyruvate therapy unless the patients are ambulatory or their pre-treatment blood levels of lactate and alanine are very high.

If the blood lactate/pyruvate ratio does not necessarily reflect the intracellular NADH/$NAD^+$ ratio, the identification of a marker other than blood lactate and pyruvate is crucial. Kami et al. found that the lysine and valine levels in media in which MELAS-mutant cybrid cells were incubated with 10 mM lactate were higher than those of controls. These increases may be because catabolisms of lysine to acetyl CoA and valine to succinyl CoA require $NAD^+$, which is deficient due to the imbalance in the NADH/$NAD^+$ ratio [15]. Plasma levels of lysine and valine in our patients, however, did not decrease with the therapy. We do not know if the levels of these amino acids may decrease with pyruvate therapy in patients with very high blood lactate levels: Koga et al. did not measure valine and lysine levels in their responsive patient [4]. Fibroblast growth factor 21 (FGF-21), a circulating hormone-like cytokine, is reported to be one of the best biomarker with high sensitivity and specificity for detecting muscle-manifesting mitochondrial respiratory chain deficiencies [16]. Although FGF-21 has higher sensitivity than lactate or lactate/pyruvate ratio to diagnose mitochondrial disease, its utility in monitoring the disease is unknown. Further study is necessary to find biomarkers to monitor the effect of pyruvate therapy biochemically.

In conclusion, as confirmed by the GMFM-88 and/or NPMDS, pyruvate therapy was safe and effective even in severely disabled patients with OXPHOS disorders, at least in the short-term. Further studies utilizing greater numbers of patients with less severe disabilities are necessary to evaluate the long-term efficacy of this treatment. The blood lactate and pyruvate levels did not correlate with the efficacy of the pyruvate therapy in our patients as has been reported in *in vitro* studies. The identification of more sensitive biomarkers that reflect the intracellular NADH/$NAD^+$ ratio or improvements in ATP production is crucial for monitoring the clinical and biochemical efficacy of this therapy.

## Conflict of interest

The authors have no conflicts of interest to disclose.

## Acknowledgments

This work was supported in part by the following grants: Grants-in-Aid for Scientific Research (A-22240072, B-21390459 and C-21590411 to MT) and a Grant-in-Aid for the Global COE (Sport Sciences for the Promotion of Active Life to Waseda University) from the Ministry of Education, Culture, Sports, Science, and Technology (to MT); grants for scientific research from The Takeda Science Foundation (to MT); Grants-in-Aid for Research on Intractable Diseases (Mitochondrial Disease) (H23-016 and H23-119 to MT; H24-005 to YK, MT and TF) from the Ministry of Health, Labor and Welfare (MHLW) of Japan; and Kawano Masanori Memorial Public Interest Incorporated Foundation for Promotion of Pediatrics (to KM).

## References

[1] M. Tanaka, Y. Nishigaki, N. Fuku, T. Ibi, K. Sahashi, Y. Koga, Therapeutic potential of pyruvate therapy for mitochondrial diseases, Mitochondrion 7 (2007) 399–401.
[2] H. Komaki, Y. Nishigaki, N. Fuku, H. Hosoya, K. Murayama, A. Ohtake, Y. Goto, H. Wakamoto, Y. Koga, M. Tanaka, Pyruvate therapy for Leigh syndrome due to cytochrome c oxidase deficiency, Biochim. Biophys. Acta 1800 (2010) 313–315.
[3] K. Saito, N. Kimura, N. Oda, H. Shimomura, T. Kumada, T. Miyajima, K. Murayama, M. Tanaka, T. Fujii, Pyruvate therapy for mitochondrial DNA depletion syndrome, Biochim. Biophys. Acta 1820 (2012) 632–636.
[4] Y. Koga, N. Povalko, K. Katayama, N. Kakimoto, T. Matsuishi, E. Naito, M. Tanaka, Beneficial effect of pyruvate therapy on Leigh syndrome due to a novel mutation in PDH E1alpha gene, Brain Dev. 34 (2012) 87–91.
[5] C. Phoenix, A.M. Schaefer, J.L. Elson, E. Morava, M. Bugiani, G. Uziel, J.A. Smeitink, D.M. Turnbull, R. McFarland, A scale to monitor progression and treatment of mitochondrial disease in children, Neuromuscul. Disord. 16 (2006) 814–820.
[6] M. Alotaibi, T. Long, E. Kennedy, S. Bavishi, The efficacy of GMFM-88 and GMFM-66 to detect changes in gross motor function in children with cerebral palsy (CP): a literature review, Disabil. Rehabil. 36 (2014) 617–627.
[7] S. Yatsuga, N. Povalko, J. Nishioka, K. Katayama, N. Kakimoto, T. Matsuishi, T. Kakuma, Y. Koga, M.S.G.i.J. Taro Matsuoka for, MELAS: a nationwide prospective cohort study of 96 patients in Japan, Biochim. Biophys. Acta 1820 (2012) 619–624.
[8] P.F. Chinnery, L.A. Bindoff, 116th ENMC international workshop: the treatment of mitochondrial disorders, 14th–16th March 2003, Naarden, the Netherlands, Neuromuscul. Disord. 13 (2003) 757–764.
[9] E. Morava, L. van den Heuvel, F. Hol, M.C. de Vries, M. Hogeveen, R.J. Rodenburg, J.A. Smeitink, Mitochondrial disease criteria: diagnostic applications in children, Neurology 67 (2006) 1823–1826.
[10] M. Linder-Lucht, V. Othmer, M. Walther, J. Vry, U. Michaelis, S. Stein, H. Weissenmayer, R. Korinthenberg, V. Mall, Gross motor function measure-traumatic brain injury study, Validation of the gross motor function measure for use in children and adolescents with traumatic brain injuries, Pediatrics 120 (2007) e880–e886.
[11] L. Nelson, H. Owens, L.S. Hynan, S.T. Iannaccone, S.G. Am, The gross motor function measure is a valid and sensitive outcome measure for spinal muscular atrophy, Neuromuscul. Disord. 16 (2006) 374–380.
[12] D. Russell, R. Palisano, S. Walter, P. Rosenbaum, M. Gemus, C. Gowland, B. Galuppi, M. Lane, Evaluating motor function in children with Down syndrome: validity of the GMFM, Dev. Med. Child Neurol. 40 (1998) 693–701.
[13] L.V. Iyer, S.M. Haley, M.P. Watkins, H.M. Dumas, Establishing minimal clinically important differences for scores on the pediatric evaluation of disability inventory for inpatient rehabilitation, Phys. Ther. 83 (2003) 888–898.
[14] M.E. Msall, K. DiGaudio, B.T. Rogers, S. LaForest, N.L. Catanzaro, J. Campbell, F. Wilczenski, L.C. Duffy, The Functional Independence Measure for Children (WeeFIM): conceptual basis and pilot use in children with developmental disabilities, Clin. Pediatr. 33 (1994) 421–430.
[15] K. Kami, Y. Fujita, S. Igarashi, S. Koike, S. Sugawara, S. Ikeda, N. Sato, M. Ito, M. Tanaka, M. Tomita, T. Soga, Metabolomic profiling rationalized pyruvate efficacy in cybrid cells harboring MELAS mitochondrial DNA mutations, Mitochondrion 12 (2012) 644–653.
[16] A. Suomalainen, J.M. Elo, K.H. Pietilainen, A.H. Hakonen, K. Sevastianova, M. Korpela, P. Isohanni, S.K. Marjavaara, T. Tyni, S. Kiuru-Enari, H. Pihko, N. Darin, K. Ounap, L.A. Kluijtmans, A. Paetau, J. Buzkova, L.A. Bindoff, J. Annunen-Rasila, J. Uusimaa, A. Rissanen, H. Yki-Jarvinen, M. Hirano, M. Tulinius, J. Smeitink, H. Tyynismaa, FGF-21 as a biomarker for muscle-manifesting mitochondrial respiratory chain deficiencies: a diagnostic study, Lancet Neurol. 10 (2011) 806–818.

Cell Metabolism
Article

# Cdk5rap1-Mediated 2-Methylthio Modification of Mitochondrial tRNAs Governs Protein Translation and Contributes to Myopathy in Mice and Humans

Fan-Yan Wei,[1,7] Bo Zhou,[1,7] Takeo Suzuki,[3] Keishi Miyata,[2] Yoshihiro Ujihara,[4] Haruki Horiguchi,[2] Nozomu Takahashi,[1] Peiyu Xie,[1] Hiroyuki Michiue,[5] Atsushi Fujimura,[5] Taku Kaitsuka,[1] Hideki Matsui,[5] Yasutoshi Koga,[6] Satoshi Mohri,[4] Tsutomu Suzuki,[3] Yuichi Oike,[2] and Kazuhito Tomizawa[1,*]

[1]Department of Molecular Physiology
[2]Department of Molecular Genetics
Faculty of Life Sciences, Kumamoto University, Kumamoto 860-8556, Japan
[3]Department of Chemistry and Biotechnology, School of Engineering, The University of Tokyo, Tokyo 113-8656, Japan
[4]First Department of Physiology, Kawasaki Medical School, Okayama 701-0192, Japan
[5]Department of Physiology, Okayama University Graduate School of Medicine, Dentistry and Pharmaceutical Sciences, Okayama 700-8558, Japan
[6]Department of Pediatrics and Child Health, Kurume University Graduate School of Medicine, Fukuoka 830-0011, Japan
[7]Co-first author
*Correspondence: tomikt@kumamoto-u.ac.jp
http://dx.doi.org/10.1016/j.cmet.2015.01.019

## SUMMARY

**Transfer RNAs (tRNAs) contain a wide variety of post-transcriptional modifications that are important for accurate decoding. Mammalian mitochondrial tRNAs (mt-tRNAs) are modified by nuclear-encoded tRNA-modifying enzymes; however, the physiological roles of these modifications remain largely unknown. In this study, we report that Cdk5 regulatory subunit-associated protein 1 (Cdk5rap1) is responsible for 2-methylthio ($ms^2$) modifications of mammalian mt-tRNAs for Ser(UCN), Phe, Tyr, and Trp codons. Deficiency in $ms^2$ modification markedly impaired mitochondrial protein synthesis, which resulted in respiratory defects in Cdk5rap1 knockout (KO) mice. The KO mice were highly susceptive to stress-induced mitochondrial remodeling and exhibited accelerated myopathy and cardiac dysfunction under stressed conditions. Furthermore, we demonstrate that the $ms^2$ modifications of mt-tRNAs were sensitive to oxidative stress and were reduced in patients with mitochondrial disease. These findings highlight the fundamental role of $ms^2$ modifications of mt-tRNAs in mitochondrial protein synthesis and their pathological consequences in mitochondrial disease.**

## INTRODUCTION

Transfer RNA (tRNA) is a key molecule in the translational apparatus to decode genetic information into proteins. A unique feature of tRNAs is the presence of a variety of chemical modifications of their nucleotides (Machnicka et al., 2013). These modifications are critical for efficient and accurate decoding (Agris, 2004; Suzuki, 2005). To date, more than 100 modified nucleotides have been identified in tRNAs from the three domains of life, indicative of the universal importance of tRNA modifications (Machnicka et al., 2013).

Given the critical roles of tRNA modifications in cells, it is not surprising that tRNA modification deficiencies have been associated with human diseases (Torres et al., 2014). Genetic variations in the gene encoding Cdk5 regulatory subunit associated protein 1-like-1 (CDKAL1), which inserts a 2-methylthio ($ms^2$) group into the $N^6$-threonylcarbamoyl adenosine ($t^6A$) of cytosolic $tRNA^{Lys}$(UUU), have been associated with the development of type 2 diabetes (Steinthorsdottir et al., 2007; Arragain et al., 2010). A deficiency in the $ms^2$ modification of $tRNA^{Lys}$(UUU) resulted in aberrant proinsulin synthesis, which ultimately led to impaired glucose metabolism and insulin secretion in Cdkal1 knockout (KO) mice and in human subjects carrying T2D-associated alleles of *CDKAL1* (Wei et al., 2011; Xie et al., 2013).

In mitochondrial tRNAs (mt-tRNAs), 15 species of modified nucleotides at 118 positions have been identified in bovine (Suzuki and Suzuki, 2014). Some of these modifications have been associated with the development of mitochondrial diseases, such as Mitochondrial myopathy, encephalopathy, lactic cidosis, stroke-like episodes (MELAS), and myoclonus epilepsy with ragged-red fibers (MERRF) (Suzuki et al., 2011). mt-$tRNA^{Leu}$ and mt-$tRNA^{Lys}$ contain 5-taurinomethyl ($\tau m^5$) and 5-taurinomethyl-2-thio ($\tau m^5 s^2$) modifications, respectively, at U34 (Yasukawa et al., 2001; Suzuki et al., 2002), and both of these modifications are critical for decoding their cognate codons (Kirino et al., 2004; Yasukawa et al., 2001). The absence of these modifications has been observed in MELAS patients carrying the A3243G mutation in mt-$tRNA^{Leu}$ and in MERRF patients carrying the A8344G mutation in mt-$tRNA^{Lys}$ (Yasukawa et al., 2001). These results suggest a critical role for mt-tRNA modifications in the pathogenesis of human diseases. Nevertheless, knowledge regarding the physiological roles of tRNA modifications is incomplete, and a complete investigation of the individual types of mt-tRNA modifications is required to fully understand the physiological function and molecular pathology of tRNA modifications in human diseases.

In mammalian mt-tRNAs, 2-methylthio-$N^6$-isopentenyl adenosine ($ms^2i^6A$) is a unique modification that is conserved in all three domains of life (Machnicka et al., 2013). In bacteria, the $ms^2$ modification of $ms^2i^6A$ contributes to accurate decoding by improving tRNA binding to codons (Urbonavicius et al., 2001; Jenner et al., 2010). However, the physiological importance of $ms^2$ modifications in mammals is unknown. We have previously shown that Cdk5rap1 might be responsible for the $ms^2$ modification of $ms^2i^6A$ because of its homology to Cdkal1, which catalyzes $ms^2t^6A$ modification (Arragain et al., 2010). Recently, Cdk5rap1 was proposed to catalyze $ms^2$ group insertion in both cytosolic RNAs and mt-tRNAs; however, the exact substrate tRNA of Cdk5rap1 in mammalian cells remains unclear (Reiter et al., 2012).

Given the exclusive mitochondrial localization of $ms^2i^6A$ in mammals and the implication of this localization in the decoding process, we hypothesize that Cdk5rap1 might specifically catalyze the $ms^2$ modification of mt-tRNAs and contribute to mitochondrial function in vivo. In this study, we validated this hypothesis through a thorough investigation of the physiological function of the $ms^2$ modification in Cdk5rap1 KO mice. Furthermore, we investigated the pathological implication and the molecular mechanism of the $ms^2$ modification in MELAS patients.

## RESULTS

### Cdk5rap1 Catalyzes the Conversion of $i^6A$ to $ms^2i^6A$ in Mitochondrial tRNAs

Based on the high homology between mammalian Cdk5rap1 and bacterial MiaB, we and another group previously showed that Cdk5rap1 might be a mammalian methylthiotransferase that catalyzes the conversion of $N^6$-isopentenyl adenosine ($i^6A$) to 2-methylthio-$N^6$-isopentenyl adenosine ($ms^2i^6A$) (Figure 1A and see Figure S1A available online; Arragain et al., 2010; Reiter et al., 2012). To investigate this hypothesis, we transformed Cdk5rap1 in MiaB-deficient bacteria (ΔMiaB), which do not contain $ms^2$ modifications. As expected, the transformation of Cdk5rap1 restored $ms^2$ modifications (Figure 1B). The conserved cysteine residues in the UPF domain and the radical SAM domain of MiaB are critical for $ms^2$ modification through their interaction with two [4Fe-4S] clusters (Forouhar et al., 2013). Similar to MiaB, the mutation of cysteine residues in the UFP domain or the radical SAM domain of Cdk5rap1 completely abolished the $ms^2$ modification (Figure 1B).

To prove that Cdk5rap1 is a mitochondrial methylthiotransferase and to identify its exact substrates, we generated Cdk5rap1 KO mice (Figures S1B–S1D). As expected, the $ms^2$ modification was completely abolished in KO mice (Figures S1E and S1F). Cdk5rap1 colocalized with Mitotracker in HeLa cells (Figure S2A). Cdk5rap1 with a deletion of mitochondrial localization signal at the N terminus exhibited cytosolic localization but retained its enzyme activity (Figures S2A and S2B). However, no $ms^2$ modification was detected in Cdk5rap1-deficient mouse embryonic fibroblast (MEF) cells expressing the cytosolic form of Cdk5rap1 (Figures S2C and S2D). These results indicate that Cdk5rap1 localizes on mitochondria and specifically modifies mt-tRNAs. To identify the exact substrate of Cdk5rap1, individual mt-tRNA was isolated from WT and KO mice and subjected to mass spectrometric analysis. The $ms^2$ modification was completely absent at A37 in mt-$tRNA^{Phe}$, mt-$tRNA^{Trp}$, mt-$tRNA^{Tyr}$, and mt-$tRNA^{Ser(UCN)}$ isolated from KO mice (Figures 1C–1F). The absence of an $ms^2$ modification did not affect the nearby $\tau m^5$ modification at U34 in mt-$tRNA^{Trp}$ (Figure S1F). These results clearly demonstrate that Cdk5rap1 is a two [4Fe-4S] cluster-containing mitochondrial methylthiotransferase that specifically converts $i^6A$ to $ms^2i^6A$ at A37 of mt-$tRNA^{Phe}$, mt-$tRNA^{Trp}$, mt-$tRNA^{Tyr}$, and mt-$tRNA^{Ser(UCN)}$ in mammalian cells.

### The $ms^2$ Modification Controls Codon-Specific Decoding Fidelity in a Translation Rate-Dependent Manner

A previous study demonstrated that the $ms^2$ group of 2-methylthio-$N^6$-hydroxyisopentenyl adenosine ($ms^2io^6A$) is critical for the accurate decoding of Tyr and Phe codons (Urbonavicius et al., 2001). To thoroughly investigate the role of $ms^2$ modifications of tRNAs during the decoding of their cognate codons, we utilized a luciferase-based reporter and transformed the plasmid into a WT strain or the ΔMiaB strain to detect frameshifting in the presence or absence of the $ms^2$ modification. The firefly luciferase gene was properly translated only when frameshifting occurred at the cognate codons read by $tRNA^{Phe}$, $tRNA^{Trp}$, $tRNA^{Tyr}$, or $tRNA^{Ser(UCN)}$ (Figure S2E). A deficiency in $ms^2$ modification induced frameshifting at Phe(TTT) and Tyr(TAT) codons (Figure 1G). Induction of protein translation by isopropyl-beta-D-thiogalactopyranoside (IPTG) exaggerated the overall frameshifting rate in both the WT and ΔMiaB strains. In addition to the Phe(TTT) and Tyr(TAT) codons, there was a significant increase in $ms^2$-dependent frameshifting at the Tyr(TAC), Ser(TCT), Ser(TCC), and Ser(TCG) codons, for which frameshifting was not observed without IPTG induction (Figures S1G–S1I). Importantly, these results show that $ms^2$-dependent frameshifting specifically occurred during the translation of wobble codons, such as Phe(TTT), Tyr(TAT), Ser(TCT), Ser(TCC), and Ser(TCG), with the exception of the Tyr(TAC) codon, but not the cognate codons, such as Phe(TTC), Ser(TCA), and Trp(TGG) (shown in red in Figures S1F–S1I). Furthermore, the $ms^2$-deficiency-evoked frameshifting was fully reversed by transformation with active Cdk5rap1, but not dominant-negative Cdk5rap1 (Figure 1G). These results demonstrate that $ms^2$ modification is critical for the accurate decoding of wobble codons corresponding to $tRNA^{Phe}$, $tRNA^{Tyr}$, or $tRNA^{Ser(UCN)}$ in a translation rate-dependent manner.

### Deficiency of the Mitochondrial $ms^2$ Modification Attenuates Mitochondrial Translation

To examine mitochondrial protein synthesis, WT or KO MEF cells were labeled with $^{35}S$-methionine for 1 hr and subjected to pulse chase. The mitochondrial protein synthesis was substantially decreased in KO MEF cells (Figure 2A). Furthermore, MEF cells were radioactively labeled and subjected to blue native PAGE to examine the formation of respiratory complexes. The incorporation of mitochondrial proteins into complexes I, III, and IV was substantially decreased in KO MEF, whereas complex V was unaffected (Figures 2B and 2C). These results suggest that the deficiency in $ms^2$ modification greatly attenuated mitochondrial protein synthesis, resulting in impaired complex assembly.

The maintenance of mitochondrial OXPHOS subunits is critical for the electron transport chain, which maintains the resting

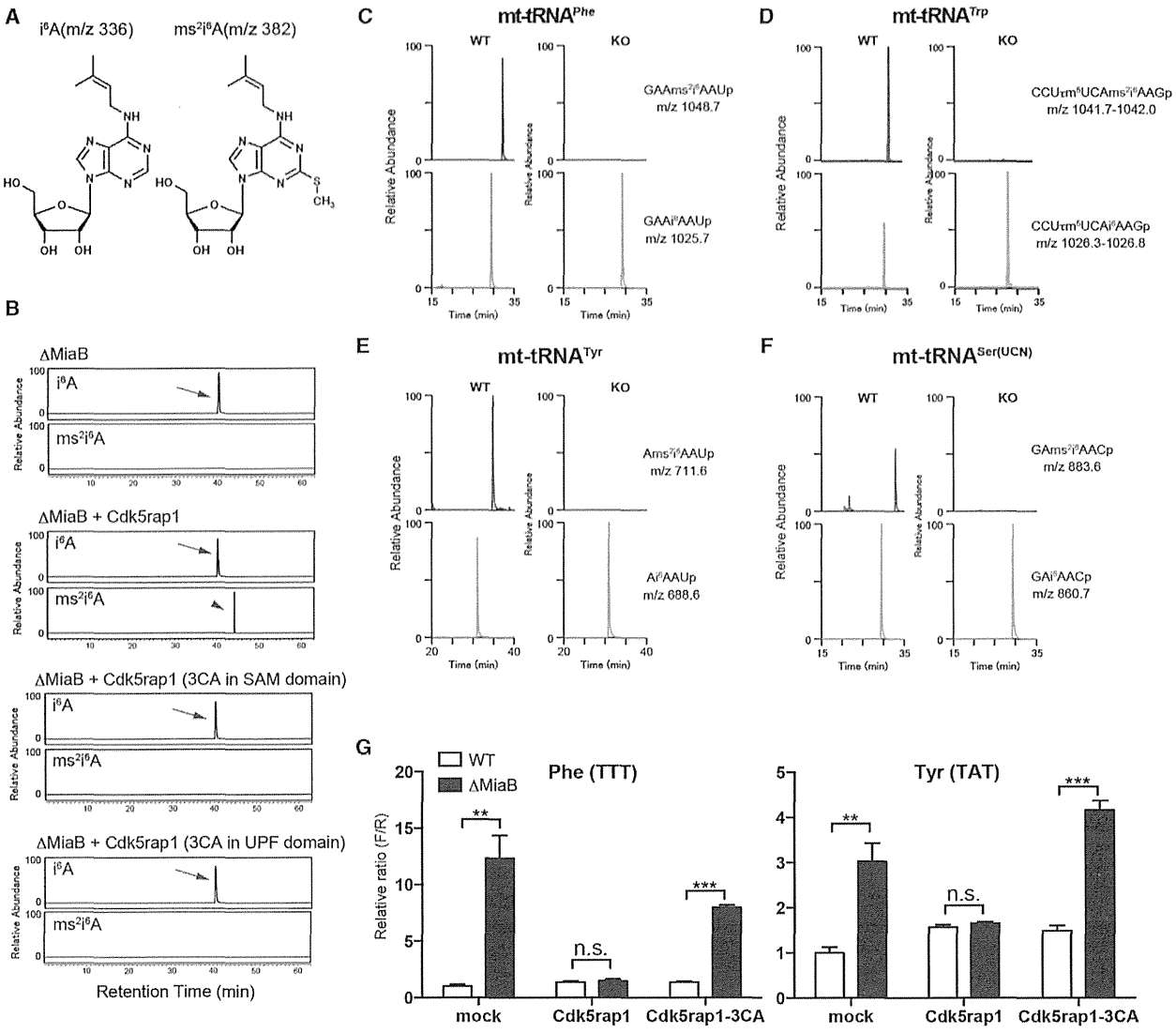


**Figure 1. Cdk5rap1 Is The Mammalian mt-tRNA Methylthiotransferase**

(A) Structures of $N^6$-isopentenyladenosine ($i^6A$) and 2-methylthio-$N^6$-isopentenyladenosine ($ms^2i^6A$) and the corresponding m/z values are shown. The $ms^2$ group ($S\text{-}CH_3$) is shown in red.

(B) GST-Cdk5rap1 or GST-Cdk5rap1 with Cys-to-Ala mutations (3CA) was transformed into the MiaB-deficient strain (ΔMiaB). The arrows and arrowhead indicate the peaks corresponding to $i^6A$ and $ms^2i^6A$, respectively.

(C–F) Examination of the $ms^2i^6A$ modification in mt-tRNA$^{Phe}$ (C), mt-tRNA$^{Trp}$ (D), mt-tRNA$^{Tyr}$ (E), and mt-tRNA$^{Ser(UCN)}$ (F) isolated from WT and KO mice by mass spectrometry. The mass chromatograms show the peaks corresponding to fragments containing $i^6A$ or $ms^2i^6A$.

(G) Frameshifting assay. WT and ΔMiaB bacteria were transformed with Cdk5rap1 or inactive Cdk5rap1 (Cdk5rap1-3CA). The relative ratio of firefly luciferase activity to renilla luciferase activity (F/R) represents the decoding error. n = 4. Data are mean ± SEM. $^{**}p < 0.01$, $^{***}p < 0.0001$.

mitochondrial membrane potential and drives respiration. We thus investigated the mitochondrial membrane potential in WT and KO MEF cells. There was a marked increase in cell populations with very low membrane potential in KO MEF cells (Figure 2D). Consequently, the oxygen consumption rate in KO cells was significantly lower than that in WT MEF cells (Figure 2E). Furthermore, the KO cells quickly lost their mitochondrial membrane potential after treatment with very low doses of rotenone and FCCP, which had little effect on WT cells (Figures 2F and 2G). These results thus demonstrate that $ms^2$ modifications of mt-tRNAs are critical for maintaining efficient mitochondrial translation and respiratory chain.

## Deficiency of Mitochondrial $ms^2$ Modification Impairs OXPHOS in Skeletal Muscle and Heart Tissue without Affecting Basal Metabolism

To investigate the physiological role of mitochondrial $ms^2$ modification, we examined the phenotype of KO mice in vivo. Despite

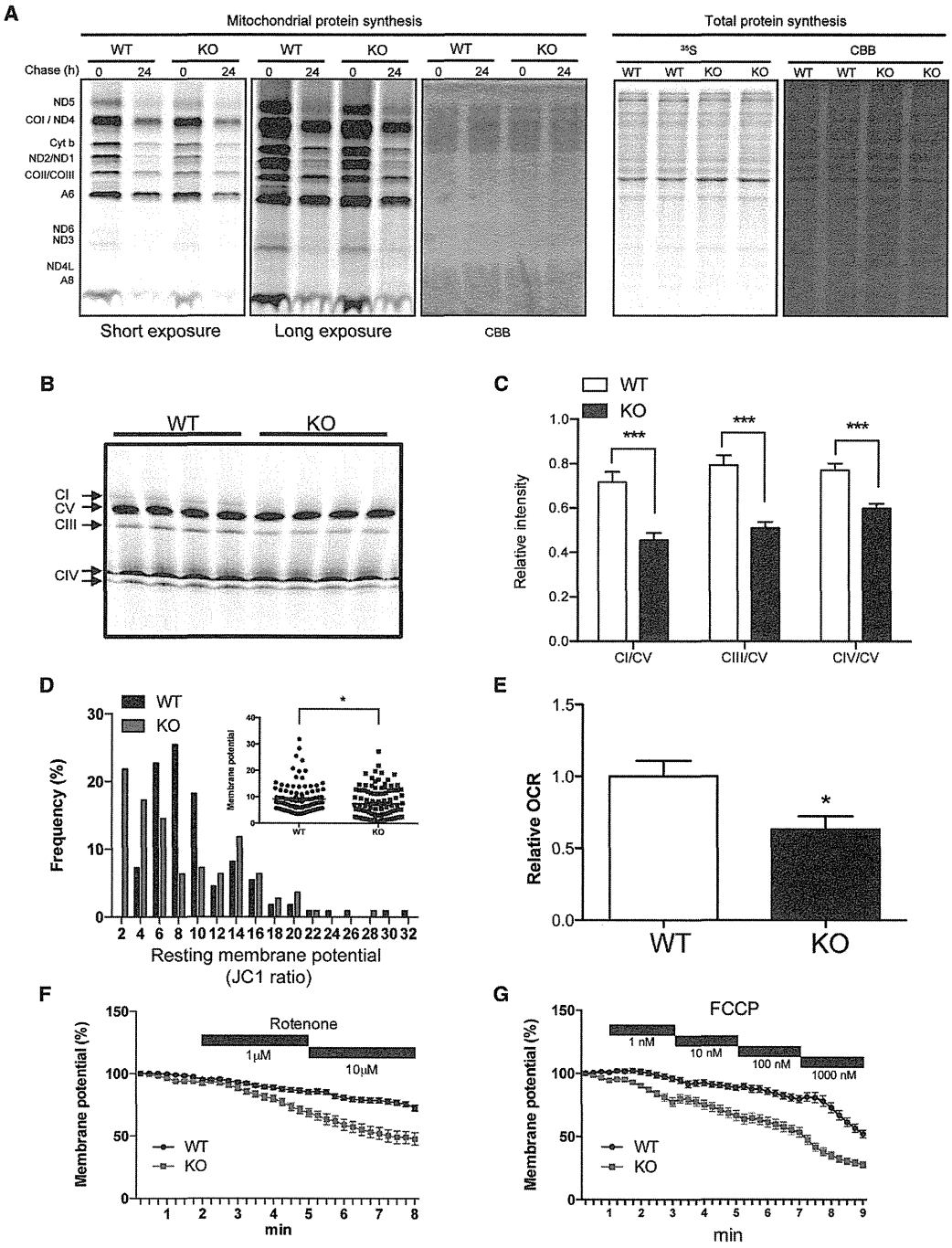


**Figure 2. Deficiency in the ms$^2$ Modifications Impaired Mitochondrial Protein Synthesis and Mitochondrial Functions**

(A) WT and KO MEF cells were labeled with $^{35}$S-Met/Cys and chased for 0 or 24 hr in the presence of emetine for measurement of mitochondrial protein synthesis (left panels). MEF cells were labeled with $^{35}$S-Met/Cys for 1 hr, and total protein synthesis was measured (right panels). CBB staining of gel was used as loading control.

(B and C) The autoradiogram of blue native PAGE shows a decrease in the incorporation of mitochondrial proteins in complexes I, III, and IV in KO MEF cells (B). The relative intensity of complex I, III, and IV versus complex V was quantified (C).

(D) The histogram and inserted graph show that KO MEF cells contain a number of mitochondria with low membrane potentials; n = 110 each.

(E) KO cells showed a significant decrease in the oxygen consumption rate (OCR); n = 10 each.

(E–G) Cells were stained with TMRM for measuring membrane potential. The relative membrane potential in the presence of rotenone (F) or FCCP (G) was analyzed; n = 66 for WT and n = 30 for KO (F); n = 43 for WT and n = 32 for KO (G). Data are mean ± SEM. *p < 0.05.

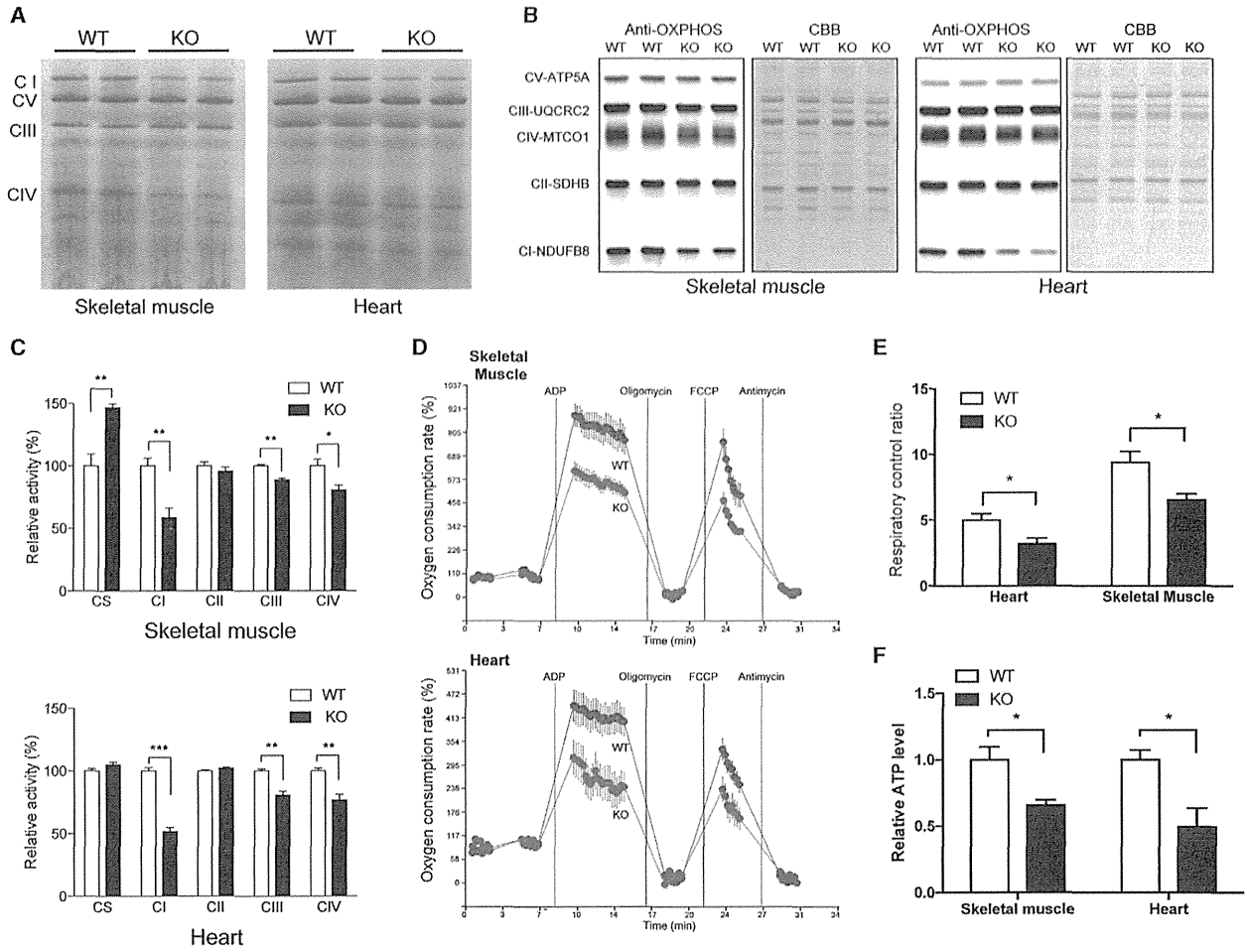


**Figure 3. The Deficiency in ms$^2$ Modification Impaired Mitochondrial Function In Vivo**

(A) Steady-state levels of complex I (CI), complex II (CIII), complex IV (CIV), and complex V (CV) in mitochondria isolated from skeletal muscle and heart tissues were examined by BN-PAGE.

(B) Steady-state levels of representative proteins of CI-CIV were examined by western blotting. CBB staining was used as loading control.

(C) The activities of CS, CI-CIV in skeletal muscle (left panel), and heart (right panel) of WT and KO mice were examined. n = 4–5.

(D and E) Respiratory coupling was decreased in Cdk5rap1-deficient mitochondria isolated from skeletal muscle and heart tissue when examined using XF24 Flux Analyzer; n = 4–5.

(F) The steady-state levels of ATP in the skeletal muscle and heart tissue of WT and KO mice were examined; n = 4 each. Data are mean ± SEM. *p < 0.05.

the mitochondrial dysfunction in KO cells, the Cdk5rap1 KO mice developed normally without obvious morphological changes in major tissues (Figures S3A and S3B). The energy expenditure and glucose metabolism in KO mice were compatible with those of WT mice (Figures S3C–S3E). Furthermore, there was no difference in neurological behaviors between KO and WT mice (Figures S3F–S3I).

Of all tissues, skeletal muscle and heart tissue are the most susceptible tissues to mitochondrial dysfunction (DiMauro and Schon, 2003). We therefore closely examined these two tissues in KO mice. Substantial decreases in the steady-state levels of complex I and IV were observed in both skeletal muscle and heart tissues of KO mice compared with WT mice, with complex I being markedly affected (Figure 3A). Accordingly, the steady-state levels of complex I and IV proteins, such as NDUFB8 and MTCO1, respectively, were markedly decreased in skeletal muscle and heart tissues of KO mice compared with WT mice (Figure 3B). As a result, complex I activity was significantly impaired in KO mice (58.6% of WT for skeletal muscle and 51.5% of WT for heart tissue) (Figure 3C). There was a mild but significant decrease in complex III and complex IV activity in KO mice (muscle: complex III, 88.8% of WT; complex IV, 80.5% of WT; heart: complex III, 80.7% of WT, complex IV, 79.8% of WT) (Figure 3C). The decrease in mitochondrial activity in the skeletal muscle of KO mice was also confirmed by cytochrome oxidase (COX) staining (Figure S3J). Accordingly, the oxygen consumption elicited by ADP and FCCP in Cdk5rap1-deficient mitochondria was significantly lower than that in WT mitochondria, indicating that electron transport and respiratory coupling were impaired in the skeletal muscle and heart tissue of KO mice (respiratory

control ratio of the hearts of WT and KO: 4.9 and 3.2, skeletal muscles of WT and KO: 9.4 and 6.5, respectively; Figures 3D and 3E). Consequently, the steady-state ATP level in skeletal muscle and heart tissue of KO mice was lower than that in WT mice (Figure 3F).

Impairment of mitochondrial function usually exaggerates mitochondrial remodeling as a compensation mechanism. There was an increase in the mitochondrial mass in the skeletal muscle of KO mice as examined by electron microscopy and Gomori Trichrome staining (Figures 4A, 4B, and S3J). Strikingly, the mitochondrial was abnormally enlarged in heart tissue of KO mice (Figures 4C and 4D). A progressive disruption of cristae was occasionally observed in the mitochondria of the cardiac muscle of KO mice (arrow in Figure 4C). Furthermore, there was a significant increase in citrate synthase activity (Figure 3C) as well as relative mtDNA content (Figure 4E) in the skeletal muscle of KO mice.

Reactive oxygen species (ROS) are byproducts of mitochondrial electron transport and mainly generated from complexes I and III (Murphy, 2009). A deficiency of complexes I and III accelerates the leakage of ROS from electron transport chain and contributes to the development of mitochondrial diseases. Given the marked decrease in complex I protein level in KO mice, we investigated ROS production in KO mice (Figure 4F). The ROS level was slightly but significantly higher in KO MEF cells than that in WT MEF cells. This finding was corroborated by a moderate increase in protein carbonylation (Figure 4G) as well as oxidative stress-related gene expression in both skeletal muscle and heart tissues of KO mice (Figure 4H).

To further investigate the impact of deficiency of $ms^2$ modification on physiological function, we examined muscular and cardiac function in vivo. However, the treadmill performance of KO mice was comparable with that of WT mice (Figure S3K). The echocardiography examination indicated that no apparent cardiac defects were present in the KO mice (Figure S3L). Taken together, these results demonstrate that the deficiency of $ms^2$ modifications in mt-tRNAs impairs mitochondrial protein synthesis, which leads to a reduction of respiratory activity and increase in ROS in skeletal muscle and heart tissue. However, considering the overall phenotypes, mice seem to tolerate an up to 50% reduction of complex I activity due to the loss of $ms^2$ modifications under sedentary conditions.

### Loss of $ms^2$ Modifications Accelerates OXPHOS Defects under Stressed Conditions

The mild phenotype of KO mice prompted us to challenge the mice with a ketogenic diet (KD; very high fat and ultra-low carbohydrate). Ketone bodies from KD bypass glycolysis and generate energy mostly through fatty acid oxidation in mitochondria (Laffel, 1999). Adaptation to this metabolic pressure is accompanied by mitochondrial rearrangement (Grimsrud et al., 2012). Therefore, it is conceivable that the accurate regulation of mitochondrial protein synthesis by $ms^2$ modification is particularly important for mitochondrial remodeling under stressed conditions.

As expected, KD treatment accelerated OXPHOS defects in the skeletal muscle and heart tissue of KO mice (Figures 4A and 4B). Complex I activity was significantly impaired in KD-fed KO mice (48.6% of the KD-fed WT for skeletal muscle and 47.7% of the KD-fed WT for heart tissue) (Figures 5A and 5B). In addition, accelerated decreases in complex III and IV activities were observed in the KD-fed KO mice (muscle: complex III, 82.9% of the KD-fed WT; complex IV, 62.9% of the KD-fed WT; heart: complex III, 75% of the KD-fed WT; complex IV, 57.8% of the KD-fed WT).

The OXPHOS defect after KD treatment exaggerated the mitochondrial remodeling pathway in both WT and KO mice. There was a ~3-fold and ~1.5-fold increase in mtDNA content in the skeletal muscle and heart tissue of both WT and KO mice fed a KD, respectively (Figure 5C). However, there was no difference in the mtDNA content in skeletal muscle and heart tissue between WT and KO mice (Figure 5C). Accordingly, subsequent electron microscopic examination revealed a marked increase in mitochondria mass (Figures 5D and 5F). In the skeletal muscles of KO mice fed a KD, mitochondrial proliferation was observed in both intermyofibrillar and subsarcolemmal mitochondria, with the latter drastically increased (Figure 5D). Importantly, KD-fed KO mice exhibited a considerable population of mitochondria with disrupted cristae in the skeletal muscle tissue (arrowheads in Figure 5D). The enlargement of mitochondria and the disruption of cristae were even more prominent in the heart tissue of KO mice fed a KD (arrows in Figure 5D). These results demonstrate that Cdk5rap1-dependent $ms^2$ modification is crucial for the maintenance of OXPHOS activity and mitochondrial morphology under stress.

The acceleration of the OXPHOS defect in KO mice may be due to the indirect lipotoxicity from the very high-fat diet. However, the body weight and serum metabolic profiles of KO mice fed a KD were the same as those of WT mice fed a KD (Figures S4A–S4C). There was no difference in the locomotor activity or energy expenditure between the WT and KO mice fed a KD (Figures S4D and S4E). Interestingly, the glucose level in the KD-fed KO mice was somewhat lower than that in the KD-fed WT mice (Figure S4F). Taken together, these results indicate that the progressive OXPHOS defects and mitochondrial degeneration in KD-fed KO mice directly resulted from a deficiency in Cdk5rap1-dependent $ms^2$ modification during mitochondrial remodeling.

### Loss of $ms^2$ Modification Accelerates Muscular and Cardiac Dysfunction under Stress

The KD-induced OXPHOS defect markedly accelerated the dysfunction of skeletal muscle and heart tissue in the KO mice. In a treadmill test, KO mice fed a KD showed a significant increase in the number of falls and became exhausted as early as 30 min into the test (Figure 5G). The KO mice also showed moderate cardiac hypertrophy, as indicated by an increase in heart volume, heart weight, and left ventricle posterior wall thickness (Figures S5A–S5C). The percentage of fractional shortening (FS%) in KO mice fed a KD was significantly lower than that in WT mice fed a KD (WT, 43% versus KO, 34%; Figure 5H). In addition to a KD-induced stress model, we utilized a transverse aortic constriction (TAC) model, which is a standard model for inducing cardiac dysfunction by pressure overload. Because the TAC model is also accompanied by global mitochondrial remodeling (Dai et al., 2012), we expected that a deficiency in $ms^2$ modification would further accelerate cardiac dysfunction. Indeed, chronic TAC resulted in a progressive cardiac hypertrophy, as indicated by an increase in heart weight and left ventricle posterior wall thickness in KO mice (WT,

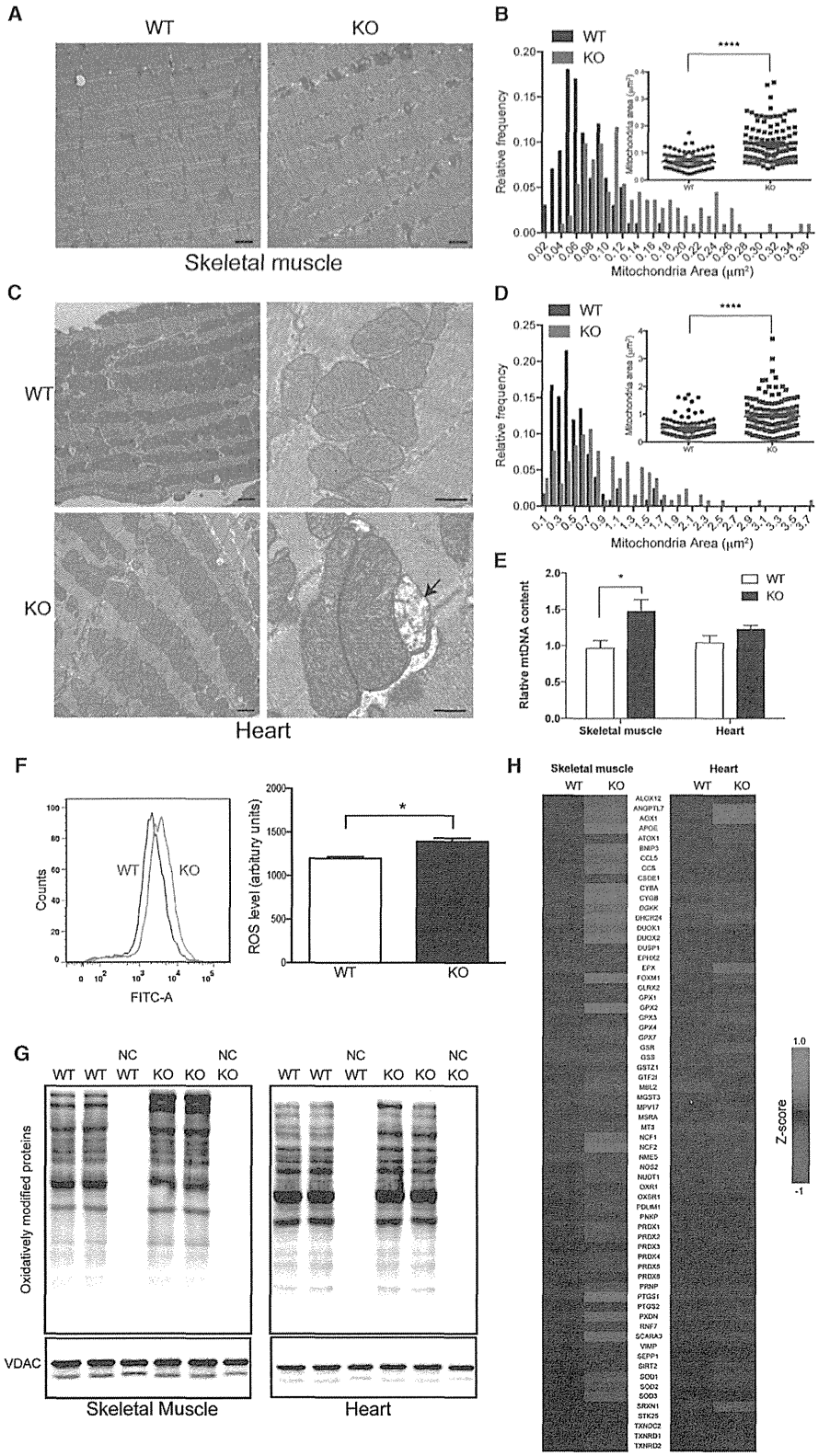


*(legend on next page)*

7.5 mg/g body weight; KO, 11.3 mg/g body weight; Figures S5A and S5D–S5F). In WT mice, the FS% dropped from 51.2% to 34.5% 1 week after TAC but was then maintained until 10 weeks (5 weeks, 32.4; 10 weeks, 31.1; Figure 5I). In contrast, the FS% in KO mice continuously decreased after TAC and eventually decreased to as low as 21.7% (Figure 5I). Further examination in isolated cardiomyocytes revealed that the cardiac dysfunction observed in the TAC model of KO mice was associated with a decrease in calcium influx and contraction rate (Figures 5J and S5G). These results demonstrate that a deficiency of the $ms^2$ modifications in mt-tRNAs can cause a catastrophic defect in muscle and heart tissue under stressed conditions.

### Deficiencies in $ms^2$ Modification Compromise the Quality of Mitochondria

Next, we investigated the molecular mechanism underlying the stress-induced acceleration of OXPHOS defects and cardiomyopathy in KO mice. Adaptation to mitochondrial stress requires coordinated protein synthesis (Dai et al., 2012). Because $ms^2$ modification controls decoding fidelity in a translation-rate-dependent manner, it is conceivable that a deficiency in $ms^2$ modification under stressed conditions might markedly compromise mitochondrial quality as well as integrity, which would result in severe OXPHOS defects and ultimately lead to myopathy and cardiac dysfunction. Indeed, a moderate increase in the complex I level was observed in WT mice treated with KD or TAC surgery (Figures 6A and 6B). In contrast, the steady-state levels of complexes I and IV levels were somewhat decreased in KD-fed and TAC KO mice when compared with NC-fed KO mice. The mitochondrial stresses increased protein carbonyltaion in both WT and KO mice. As a result, the protein carbonylation level in stressed heart tissues of KO mice was moderately higher than that in the stressed WT mice (Figure S6A). Impaired mitochondrial proteostasis exaggerates mitochondrial unfolded protein response (mt-UPR) (Durieux et al., 2011; Houtkooper et al., 2013). Accordingly, proteins involved in mtUPR, such as Yme1l1, Afg3l2, and Lonp1, were upregulated in mitochondria isolated from the hearts of KO mice treated with KD and TAC compared with WT mice (Figure 6C). Furthermore, a marked increase in polyubiquitinated proteins was observed in mitochondria isolated from the hearts of KO mice under stressed conditions (Figure 6D). Interestingly, the levels of polyubiquitination were proportional to the levels of cardiac function (FS%) in stressed KO mice (TAC > KD > NC; Figure 6D; also see Figures 5H and 5I).

Mitophagy is the hallmark of the existence of compromised mitochondria. Parkin, an E3 ubiquitin ligase, primes mitophagy by translocation to mitochondria with low membrane potentials and ubiquitination of mitochondrial proteins (Kubli and Gustafsson, 2012). Because cells with $ms^2$ modification deficiencies had a low basal mitochondrial membrane potential and were susceptible to stress-induced depolarization (Figures 2F and 2G), we hypothesized that mitochondrial stress might exaggerate the recruitment of Parkin to mitochondria and the acceleration of mitophagy in Cdk5rap1 KO cells. In KO cells treated with FCCP, most of the Parkin translocated to the mitochondria as soon as 2 hr after treatment, whereas similar translocation was not observed in WT cells treated with FCCP (Figure 6E; also see the separated imaged in Figure S6B). A number of large mitochondrial aggregates were surrounded by the autophagosomal membrane protein LC3 in KO cells treated with FCCP, which is indicative of acceleration of mitophagy (Figure 6F; also see the separated imaged in Figure S6C). Furthermore, we observed a number of degenerated mitochondria, with some mitochondria being degraded in autophagic vacuoles in KD-fed and TAC KO mice, by electron microscopic examination (Figure 6G). These results demonstrate that stress-induced mitochondrial remodeling impaired mitochondrial protein synthesis and accelerated the decomposition of respiratory complexes, which triggered the mtUPR and mitophagy in KO mice. Thus, the accumulation of compromised mitochondria ultimately contributes to the development of myopathy and cardiac dysfunction.

### Association of $ms^2$ Modification with Mitochondrial Disease

Because the pathological phenotypes of KO mice resembled those of mitochondrial disease, we speculated that $ms^2$ modification might be involved in mitochondrial disease. We investigated the $ms^2$ modification level in peripheral blood cells collected from MELAS patients who carry the A3243G mutation (Figure S7A). Because of the limited number of clinical RNA samples, we adapted the quantitative PCR-based method (Xie et al., 2013), which was originally developed to examine the $ms^2$ level of $ms^2t^6A$ in cytosolic $tRNA^{Lys(UUU)}$, to sensitively examine the $ms^2$ modification level of $ms^2i^6A$ in mt-tRNAs (Figures S7B–S7E). Strikingly, the heteroplasmy level of mutant mt-DNA was significantly correlated with the $ms^2$ modification levels of four mt-tRNAs, but not with the cytosolic tRNALys(UUU) (Figures 7A–7D and S7F). Interestingly, the mutant mtDNA level was not correlated with the expression level of *CDK5RAP1*, suggesting that the decrease in $ms^2$ modifications was not due to a deficiency in CDK5RAP1 (Figures S5D–S5G). Because the A3243G mutation is located in the mtDNA region corresponding to mt-$tRNA^{Leu(UUR)}$, the decrease in the $ms^2$ levels of $tRNA^{Trp}$, $tRNA^{Phe}$, $tRNA^{Tyr}$, and $tRNA^{Ser(UCN)}$ was likely not caused by the A3243G

**Figure 4. Aberrant Mitochondrial Morphology and ROS Metabolism in KO Mice**

(A–D) Mitochondria in skeletal muscle and heart tissue were examined by electron microscopy. KO mice exhibit disrupted mitochondrial morphology (A and C) and increased mitochondrial mass (B and D). Bars in (A) and the left panels of (C), 10 μm. Bars in the right panels of (C), 0.5 μm. WT, n = 100; KO, n = 112 in (B) and n = 126; KO, n = 132 in (D).

(E) The relative contents of mtDNA in muscle and heart tissue were examined; n = 6–9.

(F) ROS levels were analyzed by measuring the florescent intensity of CM-H2DCFDA in WT and MEF cells (left panel). The intensity was quantified (right panel); n = 3.

(G) Protein carbonylation levels were increased in the mitochondria of skeletal muscle and heart tissue in KO mice. NC, negative control.

(H) Heatmap showing the differentially regulated genes involved in oxidative stress response in skeletal muscle and heart tissue of WT and KO mice; n = 4. Data are mean ± SEM. *p < 0.5, ****p < 0.0001.

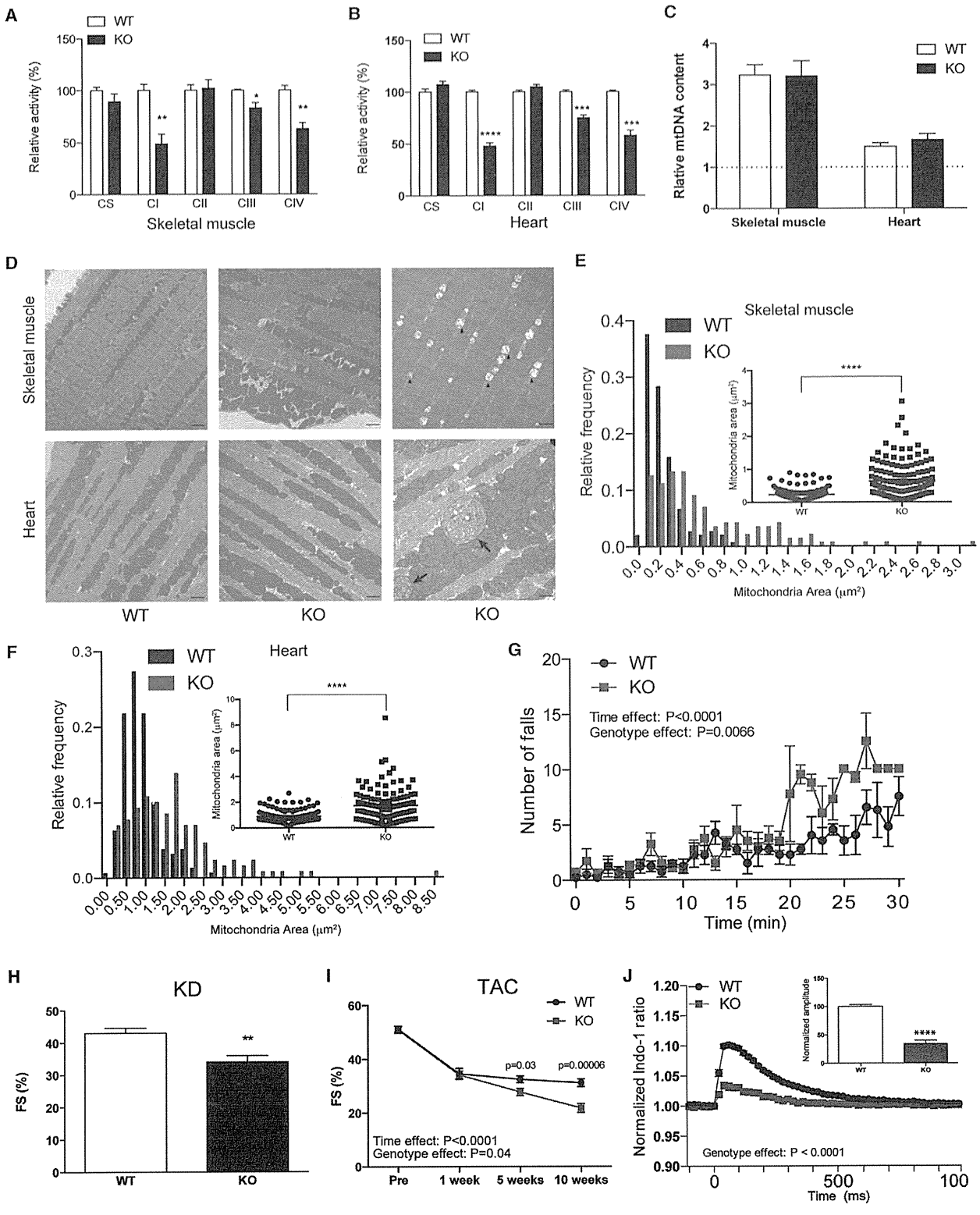


*(legend on next page)*

mutation but, rather, was due to secondary effects. Cells bearing A3243G mutations in mtDNA exhibit a marked reduction of mitochondrial protein synthesis and an increase in the oxidative stress level (Crimi et al., 2005; Ishikawa et al., 2005). Because Cdk5rap1 contains highly oxidation-sensitive [4Fe-4S] clusters (Arragain et al., 2010), we speculated that the excess oxidative stress originated from mutant mitochondria might result in a collateral inhibition of Cdk5rap1 activity. Indeed, cells treated with sublethal doses of $H_2O_2$ showed a rapid decrease in $ms^2$ modification, which was completely reversed by adding 10 mM pyruvate, which serves as an antioxidant (Figures 7E–7G). In addition, treatment of cells with an NO donor such as SNAP and NOC18 significantly reduced the $ms^2$ modification level, which was reversed by the addition of the NO scavenger PTIO (Figure 7H). Taken together, these results suggest that oxidative stress-induced decreases in $ms^2$ modifications might compromise the quality of the mitochondria and contribute to the progression of mitochondrial disease.

## DISCUSSION

### Regulation of Mitochondrial Protein Synthesis by Cdk5rap1-Mediated $ms^2$ Modification

In the present study, we revealed the important physiological functions of ancient mitochondrial $ms^2$ modifications in mice and human. Using Cdk5rap1 KO mice, we provide direct evidence that Cdk5rap1 catalyzes the $ms^2$ modifications of mt-tRNA$^{Phe}$, mt-tRNA$^{Trp}$, mt-tRNA$^{Tyr}$, and mt-tRNA$^{Ser(UCN)}$ in mammalian cells. The $ms^2$ group at the A37 of tRNA can directly participate in crossstrand stacking with the first nucleotide of the codon of the mRNA to maintain the reading frame (Jenner et al., 2010). Indeed, a deficiency in the $ms^2$ modification of $ms^2i^6A$ impaired reading frame maintenance in bacteria and caused defective mitochondrial protein synthesis in Cdk5rap1 KO mice. Interestingly, nuclear-encoded mitochondrial protein, such as NDUFB8 in complex I, was also decreased in KO mice. The indirect decrease of NDUFB8 is most likely due to the poorly assembled respiratory complexes in KO mice. A previous study has shown that a deficiency in a single subunit in complex I could compromise complex formation and cause the proteolysis of other subunits (Karamanlidis et al., 2013). Our results thus demonstrate that the $ms^2$ modification of mt-tRNAs is indispensable for mitochondrial protein synthesis and the proper assembly of respiratory complexes.

Whereas only one transcript of *Cdk5rap1* has been found in mice, multiple splicing variants of human *CDK5RAP1* are listed in the database (Figure S1A). One transcript of human *CDK5RAP1* encodes a short form of CDK5RAP1 without a mitochondrial localization signal (Q95SZ6-2 in Figure S1A), which raises the possibility that CDK5RAP1 might regulate cellular function by modifying cytosol RNAs (Reiter et al., 2012). However, there was no detectable $ms^2i^6A$ in total RNA isolated from KO MEF cells expressing the cytosolic form of Cdk5rap1 with the enzyme activity preserved. These results clearly suggest that Cdk5rap1 does not modify nuclear DNA-derived RNAs in murine cells. Furthermore, the defective mitochondrial protein synthesis observed in Cdk5rap1 KO mice may be directly caused by the loss of $ms^2$ modifications in mt-tRNAs.

### Deficiency of $ms^2$ Modification and Its Physiological Outcome

This study revealed unique phenotypic outcomes of Cdk5rap1 KO mice in response to distinct environmental conditions. Under sedentary conditions, the skeletal and cardiac functions of the Cdk5rap1 KO mice were compatible with those of the WT mice, despite the marked decrease in respiratory activities and regardless of the increase of oxidative stress. The mitochondrial dysfunction in KO mice might be compensated by the remodeling of mitonuclear protein balance, which serves as a protective mechanism by inducing mtUPR (Houtkooper et al., 2013). Indeed, in contrast to the decrease of mitochondrial protein synthesis, several cytosolic proteins appear to be upregulated in KO cells (right panels in Figure 2A). This mitonuclear protein imbalance might contribute to the upregulation of basal mtUPR in muscle and heart tissues of KO mice (Figure 6C). Furthermore, a collective increase of ROS metabolism genes, including ROS scavenger genes such as *ApoE*, *DHCR24*, and *SRXN1*, might ameliorate oxidative stress and protect the muscular and cardiac functions in KO mice. Similar to our results, previous studies have found no adverse phenotypes under basal conditions in transgenic mice with respiratory defects (Karamanlidis et al., 2013; Wenz et al., 2009). Our results thus support the current perspective that mitochondrial dysfunction, depending on its degree, may not immediately produce a pathological phenotype under sedentary conditions.

In contrast, under stressed conditions, Cdkrap1 KO mice exhibited apparent skeletal muscle and heart dysfunctions. The

**Figure 5. Mitochondrial Stresses Accelerated Myopathy and Cardiac Dysfunction in $ms^2$-Deficient Mice**

(A and B) WT and KO mice at 8 weeks old were fed for KD for 10 weeks. The relative activities of CS, CI-CIV in skeletal muscle (A), and heart (B) were examined; n = 5–7 each.

(C) The relative mtDNA contents in skeletal muscle and heart tissue of KD-fed WT and KO mice were examined; n = 6–7. The dashed lines represent the relative mtDNA content in NC-fed WT mice.

(D–F) Electron microscopy examination of skeletal muscle and heart tissue show disrupted mitochondrial architecture (D) and a marked increase in mitochondrial mass (E and F) in KD-fed KO mice. Arrowheads and arrows indicate mitochondria with abnormal cristae in skeletal muscle and heart tissues of KD-fed KO mice, respectively; bars, 10 μm; WT, n = 152; KO, n = 144 in (E) and n = 161; KO, n = 130 in (F).

(G) A treadmill test performed at the end of 10 weeks of KD feeding showed that the KD induced a higher number of falls in the KO mice during acute excise compared with the WT mice; n = 5 each.

(H) The fractional shortening (FS) rate in KO mice fed with KD for 10 weeks was significantly lower than that in KO-fed WT mice; n = 10–11.

(I) WT and KO mice at 8 weeks old were subject to TAC surgery. The KO mice showed a significant decrease in FS after TAC surgery.

(J) Cardiomyocytes were isolated from WT and KO mice 10 weeks after TAC. Calcium imaging revealed a decrease in the peak calcium influx in KO cardiomyocytes. The inserted graph shows the normalized peak amplitude of calcium influx in cardiomyocytes from WT and KO mice; n = 13 for WT and n = 6 for KO. Data are the mean ± SEM. *p < 0.05. **p < 0.01, ***p < 0.001, ****p < 0.0001.

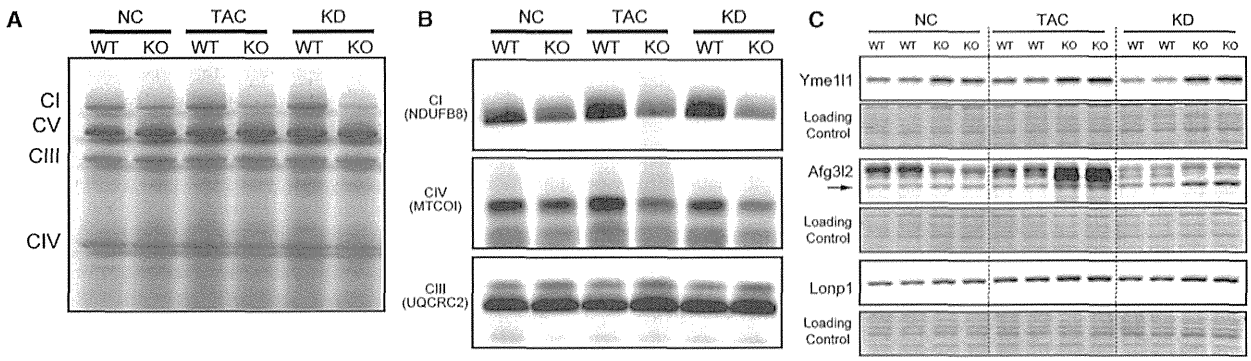


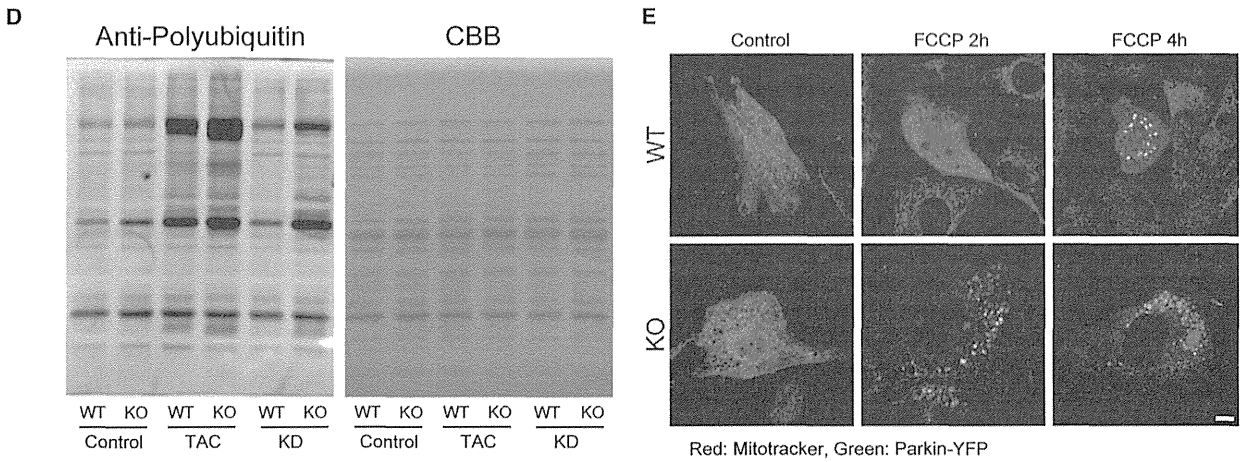


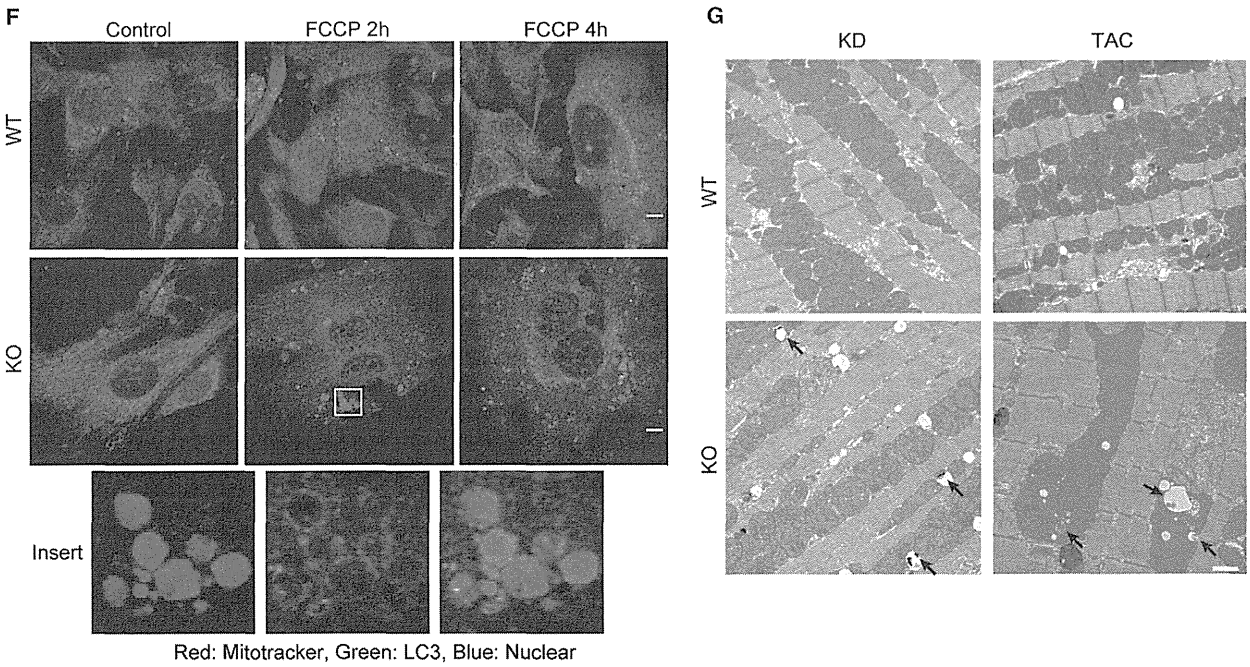


*(legend on next page)*

defective mitochondrial protein synthesis caused a marked decrease in protein levels and activities of complexes I and IV in KO mice under stressed conditions. The progressive disruption of respiratory complexes, which exaggerates mtUPR and mitophagy, thus largely compromised mitochondria quality and led to myopathy in KO mice. Recent studies have shown that Parkin-mediated mitophagy is critical for the removal of damaged mitochondria and thus protects cardiac function under stressed conditions (Hoshino et al., 2013; Chen and Dorn, 2013). However, given the observation of a number of degenerated mitochondria in KO mice (Figures 4D and 5G), the extent of mitochondria damage in KO mice was likely beyond the maintenance capacity of mitophagy, which ultimately led to catastrophic mitochondrial dysfunction and myopathy. In addition, the acceleration of complex I defect was associated with a modest increase of oxidative stress, which could trigger mtUPR and cause cytotoxicity in stressed KO mice (Runkel et al., 2013). However, compared with the progressive impairment of mitochondria quality, the degree of increase of ROS after mitochondrial stress was rather small in stressed KO mice. Our results thus suggest that ROS might also contribute to the pathogenesis, but to a limited extent. The accumulation of malfunctioning mitochondria is likely the primary cause of the progression of myopathy in KO mice.

### Regulation of $ms^2$ Modification by Oxidative Stress and Its Association with Human Disease

An important finding of this study is that the $ms^2$ modification levels were reduced in MELAS patients carrying the A3243G mutation in mt-$tRNA^{Leu}$. This result is surprising because mt-$tRNA^{Leu}$ does not contain an $ms^2$ modification. Previous studies have shown that the deficiency of taurine modification in mt-$tRNA^{Leu}$ carrying the A3243G mutation is the primary cause of MELAS (Kirino et al., 2005; Yasukawa et al., 2001). Given the significant association of the heteroplasmy level with the $ms^2$ modification level in MEALS patients, our results suggest that the myopathy in MELAS is caused not only by a decoding error at the Leu codon but also by decoding errors occurring at multiple codons, including Leu, Phe, Tyr, Trp, and Ser codons.

The reason A3243G in mt-$tRNA^{Leu}$ is associated with decreased modifications in other mt-tRNAs remains unclear. Although further studies are required to reveal the molecular mechanism, our results suggest that oxidative stress may be one of the reasons for this finding. Cdk5rap1 requires two [4Fe-4S] clusters for $ms^2$ group insertion (Forouhar et al., 2013); therefore, it is conceivable that ROS, such as $H_2O_2$ or $ONOO^-$, may oxidize these [4Fe-4S] clusters and inactivate Cdk5rap1. In support of our hypothesis, ROS-treated cells exhibited a rapid decrease in $ms^2$ modification that was effectively reversed by antioxidants. Thus, ROS generated by the mutation in mt-$tRNA^{Leu}$ might impair Cdk5RAP1-mediated $ms^2$ modification, which might further amplify mitochondrial dysfunction and ultimately accelerate myopathy in MELAS patients. In addition to mitochondrial disease, $ms^2$ modifications might be involved in a wide variety of human diseases in which ROS have been previously implicated, such as cardiac dysfunction and cancer (Schieber and Chandel, 2014).

In conclusion, this study reveals a unique quality control system in mitochondria by which the $ms^2$ modification of mt-tRNAs dynamically regulates mitochondrial protein synthesis and contributes to the development of myopathy in vivo. Our findings have important physiological implications for the basic mechanism of mitochondrial protein synthesis and provide insights into the pathological mechanism of mitochondrial disease.

## EXPERIMENTAL PROCEDURES

Please see the Supplemental Experimental Procedures for additional details.

### Animals

Cdk5rap1 KO mice were generated by crossing transgenic mice with exon 5 and 6 of *Cdk5rap1* floxed with LoxP sequence, with transgenic mice expressing Cre recombinase under the control of the CAG promoter. Mice were backcrossed to C57BL6/J mice for at least seven generations to eliminate Cre transgene and control genetic background. Littermates of WT and KO mice (8–12 weeks old) were used for experiments unless otherwise specified. Animals were housed at 25°C with 12 hr light and 12 hr dark cycles. A KD was purchased from Research Diets (D12369B). All animal procedures were approved by the Animal Ethics Committee of Kumamoto University (Approval ID, C25-163). Detailed information on genotyping can be found in the Supplemental Experimental Procedures.

### Luciferase Assay

*E. coli* colonies were transformed with plasmids encoding dual *luciferase* for detecting decoding error, *GST-Cdk5rap1*, or dominant-negative *GST-Cdk5rap1*. Colonies were cultured at 37°C, and isopropyl β-D-1-thiogalactopyranoside (IPTG) was added to the cultures at a final concentration of 1 mM. After 1 hr of incubation, the cultures were harvested for the luciferase assay using the Dual-Luciferase Reporter Assay System (Promega). Detailed procedures for detecting decoding error can be found in the Supplemental Experimental Procedures.

### Cell Culture and Transfection

Mammalian cells were grown in DMEM high-glucose medium (GIBCO) supplemented with 10% fetal bovine serum (FBS, HyClone) at 37°C and 5% $CO_2$.

**Figure 6. The Deficiency in $ms^2$ Modification Compromises Mitochondrial Protein Quality under Stressed Conditions**

(A) Steady-state levels of CI, CIII, CIV, and CV in heart tissue in WT and KO mice treated with NC, KD, and TAC surgery were examined by BN-PAGE.

(B) The steady-state levels of CI protein NDUFB8, CIV protein MTCOI, and CIII protein UQCRC2 in heart tissue in WT and KO mice treated with NC, KD, and TAC surgery were examined by BN-PAGE followed by western blotting. UQCRC2 was used as a loading control.

(C) The protein levels of Yme1l1, Afg 3l2, and Lonp1 were examined in heart tissues from WT and KO mice treated with NC, KD, and TAC surgery. Membranes stained with CBB were used as a loading control.

(D) Enhanced polyubiquitination was observed in the mitochondria in the hearts of KO mice under each stress.

(E) WT and KO cells transfected with Parkin-YFP were treated with 10 μM FCCP for 2 and 4 hr; bar, 10 μm.

(F) WT and KO cells were treated with 10 μM FCCP for 2 and 4 hr. The cells were then stained with an anti-LC3 antibody and Mitotracker. The inserted box shows mitochondria surrounded by the LC3 protein and is magnified in the bottom panels; bar, 10 μm.

(G) Electron microscopy of mitochondria in heart tissue from WT and KO mice treated with KD or TAC surgery. Arrows indicate the autophagic vacuoles; bar, 10 μm.

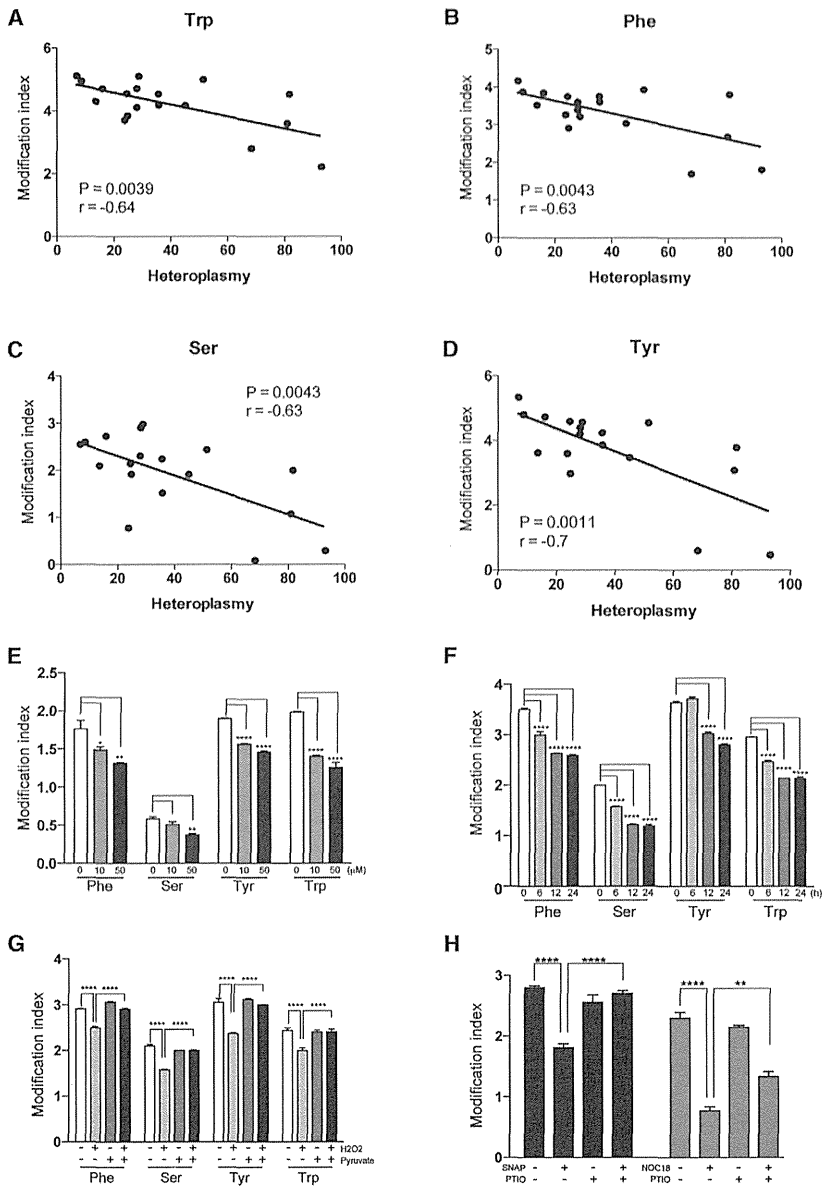


**Figure 7. Association of ms$^2$ Modifications with MELAS**

(A–D) Negative correlation of the ms$^2$ modification level of mt-tRNA$^{Trp}$ (A), mt-tRNA$^{Phe}$ (B), mt-tRNA$^{Ser(UCN)}$ (C), or mt-tRNA$^{Tyr}$ (D) with the heteroplasmy level in MELAS patients; n = 18 each.

(E) Treatment with $H_2O_2$ reduced the level of ms$^2$ modification of mt-tRNAs in HeLa cells. Cells were treated with 10 μM or 50 μM $H_2O_2$ for 24 hr, and the ms$^2$ modification levels were examined by qPCR; n = 4 each.

(F) Time-dependent decreases in ms$^2$ modification after $H_2O_2$ treatment in HeLa cells. Cells were treated with 50 μM $H_2O_2$ for 6, 12, and 24 hr; n = 4 each.

(G) HeLa cells were treated with 50 μM $H_2O_2$ for 24 hr in the presence or absence of 10 mM pyruvate. The decrease in the ms$^2$ modification level was prevented by pyruvate; n = 4 each.

(H) HeLa cells were treated with NO donors, 100 μM SNAP or 100 μM NOC18 for 24 hr in the presence or absence of PTIO. The ms$^2$ modification level of mt-tRNA$^{Trp}$ was examined by qPCR; n = 4 each. Data are the mean ± SEM. *p < 0.05. **p < 0.01, ****p < 0.0001.

Transfection of the plasmid DNA was performed with Lipofectamine 2000 (Invitrogen).

### Oxygen Consumption

The oxygen consumption rate in MEF cells and intact mitochondria was measured using an XF24 Analyzer (Seahorse Bioscience). The oxygen consumption rate was normalized to the total protein concentration for measurement in cells. Detailed procedures for the respiratory assay can be found in the Supplemental Experimental Procedures.

### Gene Expression Assay

RNA was extracted from tissues using Trizol (Invitrogen) following the manufacturer's instructions. Quantitative PCR (qPCR) was performed using SYBR Premix Ex Taq (TAKARA). For examination of the expression levels of oxidative response genes, the results were normalized to the geometric mean of multiple reference genes (Hprt1, RPL13A, B2M, GAPDH, ACT). Then, a Z-transformation was applied to the results to calculate the *Z* score and construct a heatmap (Cheadle et al., 2003). The sequences of primers used can be found in the Supplemental Experimental Procedures.

### Analysis of tRNA Modification

Total RNAs were isolated from bacteria and tissues using Trizol reagent (Invitrogen). RNA was digested with Nuclease P1 (Sigma) and subjected to mass spectrometry (Agilent 6460). For detecting tRNA modification using the qPCR-based method, we adapted a protocol described previously (Xie et al., 2013). Detailed procedures for the mass spectrometry and qPCR method can be found in the Supplemental Experimental Procedures. To measure the tRNA modification level in blood samples, blood samples were collected from MELAS patients using standard procedures approved by Kurume University (IRB#9715).

### ATP Measurement

Small pieces of skeletal muscle and heart tissue were immediately dissected after sacrificing mice and snap frozen in liquid nitrogen until measurement. ATP was measured using the ATP Bioluminescence Assay Kit following the manufacturer's protocol (TA100, WAKO). The luminescence was measured using a Centro XS$^3$ LB960 (Berthold) and normalized to total protein concentration.

### Cardiac Function Examination

Echocardiographs were examined in M-mode while the mice were under anesthesia using the Vevo2100 system (Fujifilm VisualSonics, Inc.) according to the manufacturer's instructions.

### Statistical Analysis

Statistical analyses were performed using Prism 6 Software (GraphPad Software). An unpaired Student t test was used to test the differences between two groups. Analysis of variance (one-way ANOVA or two-way ANOVA) was used to test the difference among multiple groups followed by a post hoc examination of the p value between two groups. A two-tailed p value of 0.05 was considered statistically significant.

## SUPPLEMENTAL INFORMATION

Supplemental Information includes seven figures and Supplemental Experimental Procedures and can be found with this article at http://dx.doi.org/10.1016/j.cmet.2015.01.019.

## AUTHOR CONTRIBUTIONS

F.-Y.W. and K.T. designed the experiments and wrote the manuscript. F.-Y.W. and B.Z. performed the experiments. Takeo Suzuki and Tsutomu Suzuki performed the mass spectrometry experiments. H.H., K.M., and Y.O. performed cardiac examinations. Y.U. and S.M. performed TAC surgery and cardiac examinations. H. Michiue, A.F., and H. Matsui performed electron microscopy. Y.K. provided the blood samples. N.T., P.X., and T.K. performed the qPCR-based examination of tRNA modifications.

## ACKNOWLEDGMENTS

We thank Nobuko Maeda for the technical assistance. This work was supported by a Grant-in-Aid for Scientific Research from the Ministry of Education, Culture, Sports, Science, and Technology of Japan, by the Japan Society for the Promotion of Science (JSPS) through its "Funding Program for Next Generation World-Leading Researchers," and by the Takeda Science Foundation.

Received: September 5, 2014
Revised: November 24, 2014
Accepted: January 26, 2015
Published: March 3, 2015

## REFERENCES

Agris, P.F. (2004). Decoding the genome: a modified view. Nucleic Acids Res. *32*, 223–238.

Arragain, S., Handelman, S.K., Forouhar, F., Wei, F.Y., Tomizawa, K., Hunt, J.F., Douki, T., Fontecave, M., Mulliez, E., and Atta, M. (2010). Identification of eukaryotic and prokaryotic methylthiotransferase for biosynthesis of 2-methylthio-$N^6$-threonylcarbamoyladenosine in tRNA. J. Biol. Chem. *285*, 28425–28433.

Cheadle, C., Vawter, M.P., Freed, W.J., and Becker, K.G. (2003). Analysis of microarray data using Z score transformation. J. Mol. Diagn. *5*, 73–81.

Chen, Y., and Dorn, G.W., 2nd. (2013). PINK1-phosphorylated mitofusin 2 is a Parkin receptor for culling damaged mitochondria. Science *340*, 471–475.

Crimi, M., Bordoni, A., Menozzi, G., Riva, L., Fortunato, F., Galbiati, S., Del Bo, R., Pozzoli, U., Bresolin, N., and Comi, G.P. (2005). Skeletal muscle gene expression profiling in mitochondrial disorders. FASEB J. *19*, 866–868.

Dai, D.F., Hsieh, E.J., Liu, Y., Chen, T., Beyer, R.P., Chin, M.T., MacCoss, M.J., and Rabinovitch, P.S. (2012). Mitochondrial proteome remodelling in pressure overload-induced heart failure: the role of mitochondrial oxidative stress. Cardiovasc. Res. *93*, 79–88.

DiMauro, S., and Schon, E.A. (2003). Mitochondrial respiratory-chain diseases. N. Engl. J. Med. *348*, 2656–2668.

Durieux, J., Wolff, S., and Dillin, A. (2011). The cell-non-autonomous nature of electron transport chain-mediated longevity. Cell *144*, 79–91.

Forouhar, F., Arragain, S., Atta, M., Gambarelli, S., Mouesca, J.M., Hussain, M., Xiao, R., Kieffer-Jaquinod, S., Seetharaman, J., Acton, T.B., et al. (2013). Two Fe-S clusters catalyze sulfur insertion by radical-SAM methylthiotransferases. Nat. Chem. Biol. *9*, 333–338.

Grimsrud, P.A., Carson, J.J., Hebert, A.S., Hubler, S.L., Niemi, N.M., Bailey, D.J., Jochem, A., Stapleton, D.S., Keller, M.P., Westphall, M.S., et al. (2012). A quantitative map of the liver mitochondrial phosphoproteome reveals post-translational control of ketogenesis. Cell Metab. *16*, 672–683.

Hoshino, A., Mita, Y., Okawa, Y., Ariyoshi, M., Iwai-Kanai, E., Ueyama, T., Ikeda, K., Ogata, T., and Matoba, S. (2013). Cytosolic p53 inhibits Parkin-mediated mitophagy and promotes mitochondrial dysfunction in the mouse heart. Nat. Commun. *4*, 2308.

Houtkooper, R.H., Mouchiroud, L., Ryu, D., Moullan, N., Katsyuba, E., Knott, G., Williams, R.W., and Auwerx, J. (2013). Mitonuclear protein imbalance as a conserved longevity mechanism. Nature *497*, 451–457.

Ishikawa, K., Kimura, S., Kobayashi, A., Sato, T., Matsumoto, H., Ujiie, Y., Nakazato, K., Mitsugi, M., and Maruyama, Y. (2005). Increased reactive oxygen species and anti-oxidative response in mitochondrial cardiomyopathy. Circ. J. *69*, 617–620.

Jenner, L.B., Demeshkina, N., Yusupova, G., and Yusupov, M. (2010). Structural aspects of messenger RNA reading frame maintenance by the ribosome. Nat. Struct. Mol. Biol. *17*, 555–560.

Karamanlidis, G., Lee, C.F., Garcia-Menendez, L., Kolwicz, S.C., Jr., Suthammarak, W., Gong, G., Sedensky, M.M., Morgan, P.G., Wang, W., and Tian, R. (2013). Mitochondrial complex I deficiency increases protein acetylation and accelerates heart failure. Cell Metab. *18*, 239–250.

Kirino, Y., Yasukawa, T., Ohta, S., Akira, S., Ishihara, K., Watanabe, K., and Suzuki, T. (2004). Codon-specific translational defect caused by a wobble modification deficiency in mutant tRNA from a human mitochondrial disease. Proc. Natl. Acad. Sci. USA *101*, 15070–15075.

Kirino, Y., Goto, Y., Campos, Y., Arenas, J., and Suzuki, T. (2005). Specific correlation between the wobble modification deficiency in mutant tRNAs and the clinical features of a human mitochondrial disease. Proc. Natl. Acad. Sci. USA *102*, 7127–7132.

Kubli, D.A., and Gustafsson, Å.B. (2012). Mitochondria and mitophagy: the yin and yang of cell death control. Circ. Res. *111*, 1208–1221.

Laffel, L. (1999). Ketone bodies: a review of physiology, pathophysiology and application of monitoring to diabetes. Diabetes Metab. Res. Rev. *15*, 412–426.

Machnicka, M.A., Milanowska, K., Osman Oglou, O., Purta, E., Kurkowska, M., Olchowik, A., Januszewski, W., Kalinowski, S., Dunin-Horkawicz, S., Rother, K.M., et al. (2013). MODOMICS: a database of RNA modification pathways—2013 update. Nucleic Acids Res. *41* (Database issue), D262–D267.

Murphy, M.P. (2009). How mitochondria produce reactive oxygen species. Biochem. J. *417*, 1–13.

Reiter, V., Matschkal, D.M., Wagner, M., Globisch, D., Kneuttinger, A.C., Müller, M., and Carell, T. (2012). The CDK5 repressor CDK5RAP1 is a methylthiotransferase acting on nuclear and mitochondrial RNA. Nucleic Acids Res. *40*, 6235–6240.

Runkel, E.D., Liu, S., Baumeister, R., and Schulze, E. (2013). Surveillance-activated defenses block the ROS-induced mitochondrial unfolded protein response. PLoS Genet. *9*, e1003346.

Schieber, M., and Chandel, N.S. (2014). ROS function in redox signaling and oxidative stress. Curr. Biol. *24*, R453–R462.

Steinthorsdottir, V., Thorleifsson, G., Reynisdottir, I., Benediktsson, R., Jonsdottir, T., Walters, G.B., Styrkarsdottir, U., Gretarsdottir, S., Emilsson, V., Ghosh, S., et al. (2007). A variant in CDKAL1 influences insulin response and risk of type 2 diabetes. Nat. Genet. *39*, 770–775.

Suzuki, T. (2005). Biosynthesis and function of tRNA wobble modifications. Topics Curr. Genet. *12*, 24–69.

Suzuki, T., and Suzuki, T. (2014). A complete landscape of post-transcriptional modifications in mammalian mitochondrial tRNAs. Nucleic Acids Res. *42*, 7346–7357.

Suzuki, T., Suzuki, T., Wada, T., Saigo, K., and Watanabe, K. (2002). Taurine as a constituent of mitochondrial tRNAs: new insights into the functions of taurine and human mitochondrial diseases. EMBO J. *21*, 6581–6589.

Suzuki, T., Nagao, A., and Suzuki, T. (2011). Human mitochondrial tRNAs: biogenesis, function, structural aspects, and diseases. Annu. Rev. Genet. *45*, 299–329.

Torres, A.G., Batlle, E., and Ribas de Pouplana, L. (2014). Role of tRNA modifications in human diseases. Trends Mol. Med. *20*, 306–314.

Urbonavicius, J., Qian, Q., Durand, J.M., Hagervall, T.G., and Björk, G.R. (2001). Improvement of reading frame maintenance is a common function for several tRNA modifications. EMBO J. *20*, 4863–4873.

Wei, F.Y., Suzuki, T., Watanabe, S., Kimura, S., Kaitsuka, T., Fujimura, A., Matsui, H., Atta, M., Michiue, H., Fontecave, M., et al. (2011). Deficit of tRNA(Lys) modification by Cdkal1 causes the development of type 2 diabetes in mice. J. Clin. Invest. *121*, 3598–3608.

Wenz, T., Luca, C., Torraco, A., and Moraes, C.T. (2009). mTERF2 regulates oxidative phosphorylation by modulating mtDNA transcription. Cell Metab. *9*, 499–511.

Xie, P., Wei, F.Y., Hirata, S., Kaitsuka, T., Suzuki, T., Suzuki, T., and Tomizawa, K. (2013). Quantitative PCR measurement of tRNA 2-methylthio modification for assessing type 2 diabetes risk. Clin. Chem. *59*, 1604–1612.

Yasukawa, T., Suzuki, T., Ishii, N., Ohta, S., and Watanabe, K. (2001). Wobble modification defect in tRNA disturbs codon-anticodon interaction in a mitochondrial disease. EMBO J. *20*, 4794–4802.